NEOPLASIA
www.neoplasia.com

Volume 16 Number 1 January 2014 pp. 43–72 43

Doubling Down on the PI3K-AKT-mTOR Pathway Enhances the Antitumor Efficacy of PARP Inhibitor in Triple Negative Breast Cancer Model beyond BRCA-ness[1,2]

Pradip De[*,†], Yuling Sun[*], Jennifer H. Carlson[*], Lori S. Friedman[‡], Brian R. Leyland-Jones[*,†] and Nandini Dey[*,†]

[*]Department of Molecular and Experimental Medicine, Avera Cancer Institute, Sioux Falls, SD; [†]Department of Internal Medicine, University of South Dakota, Vermillion, SD; [‡]Genentech, South San Francisco, CA

Abstract

Phosphoinositide 3-kinase (PI3K) pathway, in addition to its pro-proliferative and antiapoptotic effects on tumor cells, contributes to DNA damage repair (DDR). We hypothesized that GDC-0980, a dual PI3K-mammalian target of rapamycin (mTOR) inhibitor, would induce an efficient antitumor effect in BRCA-competent triple negative breast cancer (TNBC) model when combined with ABT888 and carboplatin. Mechanism-based *in vitro* studies demonstrated that GDC-0980 treatment alone or in combination led to DNA damage (increased pγH2AX^{S139}; Western blot, immunofluorescence), gain in poly ADP-ribose (PAR), and a subsequent sensitization of BRCA-competent TNBC cells to ABT888 plus carboplatin with a time-dependent 1) decrease in proliferation signals (pAKT$^{T308/S473}$, pP70S6K$^{T421/S424}$, pS6RP$^{S235/236}$), PAR/poly(ADP-ribose) polymerase (PARP) ratios, PAR/pγH2AX ratios, live/dead cell ratios, cell cycle progression, and three-dimensional clonogenic growths and 2) increase in apoptosis markers (cleaved caspases 3 and 9, a pro-apoptotic BH3-only of Bcl-2 family (BIM), cleaved PARP, annexin V). The combination was effective *in vitro* in BRCA–wild-type *PIK3CA*-H1047R–mutated BT20 and PTEN-null HCC70 cells. The combination blocked the growth of established xenograft tumors by 80% to 90% with a concomitant decrease in tumor Ki67, CD31, phosphorylated vascular endothelial growth factor receptor, pS6RP$^{S235/236}$, and p4EBP1$^{T37/46}$ as well as an increase in cleaved caspase 3 immunohistochemistry (IHC) levels. Interestingly, a combination with GDC-0941, a pan-PI3K inhibitor, failed to block the tumor growth in MDA-MB231. Results demonstrate that the dual inhibition of PI3K and mTOR regulates DDR. In a BRCA-competent model, GDC-0980 enhanced the antitumor activity of ABT888 plus carboplatin by inhibiting both tumor cell proliferation and tumor-induced angiogenesis along with an increase in the tumor cell apoptosis. This is the first mechanism-based study to demonstrate the integral role of the PI3K-AKT-mTOR pathway in DDR-mediated antitumor action of PARP inhibitor in TNBC.

Neoplasia (2014) 16, 43–72

Abbreviations: *BRCA1* and *BRCA2*, human genes that produce tumor suppressor proteins [These proteins help repair damaged DNA. Together, *BRCA1* and *BRCA2* mutations account for about 20% to 25% of hereditary breast cancers and about 5% to 10% of all breast cancers (from National Cancer Institute web page).]; DDR, DNA damage repair; DSBs, double-strand breaks; PARP, poly(ADP-ribose) polymerase (DNA damage repair enzyme); SSBs, single-strand breaks; TNBC, triple negative breast cancer

Address all correspondence to: Nandini Dey, PhD, Senior Scientist, Department of Molecular and Experimental Medicine, Avera Cancer Institute, Sioux Falls, SD, and Assistant Professor, Department of Internal Medicine, University of South Dakota. E-mail: nandini.dey@Avera.org or Brian R. Leyland-Jones, MD, PhD, Vice President, Molecular and Experimental Medicine, 1000 E 23rd Street, Suit 320, Sioux Falls, SD 57105. E-mail: brian.leyland-jones@Avera.org

[1]This study was supported by research funding from Edith Sanford Breast Cancer, Sanford Research/University of South Dakota and facilities and cores of the Sanford Research.
[2]This article refers to supplementary materials, which are designated by Figures W1 to W5 and Movies W1 to W4 and are available online at www.neoplasia.com.
Received 25 September 2013; Revised 5 December 2013; Accepted 19 December 2013

DOI 10.1593/neo.131694

Introduction

Poly(ADP-ribose) polymerase (PARP) has been the most promising target in the triple negative (TN) subset of breast cancer (BC), the most aggressive BC subset with limited options for a targeted therapy [1–6]. As a nick-sensor, PARP binds to and initiates the repair of DNA single-strand breaks (SSBs). A failure to repair these events leads to persistent SSBs, which otherwise gets converted into potentially clastogenic or lethal double-strand breaks (DSBs) at the "replication fork." DSBs are corrected by either homologous recombination (HR) or nonhomologous end joining (NHEJ). However, DNA repair by HR, but not by NHEJ, is reported to be elevated in BC cells [7]. Thus, PARP inhibitors (PARPi) have potential chemosensitizing, radiosensitizing, and antineoplastic activities [8–10]. PARPi have so far shown the most promising effects in the BRCA1/2-deficient patient population, owing to their ability to induce "synthetic lethality" [9,11,12], mediated through the accumulation of structural DNA lesions, the correction of which requires a coordinated action of a number of DNA damage repair (DDR) enzymes. However, BRCA1/2 mutations account for only 2% to 3% of all BCs, and thus, a significant percentage of the population of TN and/or basal-type BC patients remains BRCA competent [5] for whom PARPi as a single agent offers a very limited therapeutic opportunity [3,13]. To date, studies to extend the use of PARPi outside the "BRCA box" were inadequate and inconclusive [14].

The phosphoinositide 3-kinase (PI3K) enzyme contributes to repair of DSB in addition to its role in pro-proliferative and antiapoptotic functions in tumor cells [15]. Recently, the PI3K enzyme has been demonstrated to play a critical role in RAD51 recruitment [16]. The PI3K signaling pathway has been reported to maintain HR steady state and stabilize and preserve DSB repair by interacting with the HR complex [15]. Suppression of PI3K function has been shown to impair HR [17]. Mammalian target of rapamycin (mTOR), as a family member of PI3K-related protein kinases including ATM, ATR, and DNA-PK, was also reported to be involved in DDR [18,19]. The kinase activity of mTOR has been particularly known to integrate nutrient/energy signaling with that of growth factor signaling [20–22] in highly dividing tumor cells (TNBC cells characteristically exhibit a high mitotic index), and RAD001 has been shown to sensitize tumor cells to cisplatin-mediated DNA damage–induced apoptosis [19]. Recently, the dual PI3K-mTOR inhibitor NVP-BEZ235 has been reported to inhibit ATM- and DNA-dependent protein kinase, catalytic subunit (DNA-PKcs)–mediated DNA damage responses in glioblastoma multiforme (GBM) cell lines [23].

PARPi are clinically effective in BRCA1/2-incompenent patients. However, there exists a larger percentage of BRCA-competent TN and/or basal-type BC patients who are outside the "BRCA box." Here, we identified, for the first time, the anti-DDR effect of GDC-0980 and demonstrated that this effect brings an effective antitumor efficacy in a BRCA-competent TNBC model when combined with ABT888 in the presence of carboplatin. In a BRCA-competent model, GDC-0980 enhanced the antitumor activity of ABT888, in the presence of carboplatin, by inhibiting DDR in addition to its antiproliferative and proapoptotic functions. Considering the importance of PARP as a target in TNBC, and the existence of a large percentage of BRCA-competent TN and/or basal-type BC patients, our data extend the realm of use of PARPi in combination with dual PI3K-mTOR inhibitor plus carboplatin beyond the "BRCA box," which merits further investigation to test this combination in future phase I/II clinical trials.

The corollary that emerged from the concept of "synthetic lethality" proposed by Tutt et al. [9], in the context of PARPi, was that *a tumor cell with high mitotic rates has an inherent limit to withstand the extent of DNA-damage which is otherwise required to be corrected before the cell enters mitosis*. Because tumor cells of TNBC exhibit high mitotic indices, the reliance of these cells on DDR should be high. In addition to the error-free maintenance of tumor cell DNA, the high mitotic rate in these TNBC cells with p53-null background demand 1) a higher rate of cell cycle, 2) a reduced level of apoptosis, and 3) a challenging nutritional/metabolic/protein translational state. In this study, we attempted to exploit these characteristics of a BRCA-competent TNBC tumor cell line to induce a higher magnitude of cell kill *in vitro* and *in vivo* by choosing a combination of GDC-0980 with ABT888 plus carboplatin. We *hypothesized* that a dual PI3K-mTOR kinase inhibitor, in combination with PARPi plus carboplatin, would 1) sensitize a tumor cell to PARPi (ABT888) through inhibiting/retarding the capacity of the tumor cell to carry out PI3K-dependent DDR (endogenous as well as inflicted by carboplatin) and 2) inhibit growth of the tumor by counteracting the PI3K-mTOR–mediated survival/proliferative signals from cell surface receptor(s) and nutrient milieu of the cell. Recently, proteomic markers of DNA repair and PI3K pathway activation have been shown to predict response to the PARPi BMN 673 in small cell lung cancer [24]. In their study, Cardnell et al. demonstrated that sensitivity to PARPi was associated with elevated baseline expression levels of several DNA repair proteins, whereas greater drug resistance was observed in small cell lung cancer models with baseline activation of the PI3K-mTOR pathway. These observations complement our work in which PI3K-mTOR inhibition has been shown to sensitize BRCA1-competent TNBC model to PARP inhibition, suggesting cooperation between DDR and PI3K pathway.

The armory of "targeted therapy" for the treatment of TNBC has been inadequate because of the inherent complexity of TNBC biology, the lack of "traditional" therapeutic targets, and the identification of pathway-specific targets [25]. Recently, we have identified the role of the Wnt–β-catenin pathway in the context of metastasis in TNBC and revealed a mechanistic relationship between this pathway and the loss of tumor suppressor PTEN [26,27]. Here, we report for the *first* time that growth of a BRCA-competent TNBC tumor was blocked by a combination treatment of a dual PI3K-mTOR inhibitor with a PARPi in the presence of carboplatin. Our data identify *the inhibition of DDR as another mode of action of GDC-0980* and demonstrate that when combined with carboplatin plus ABT888, GDC-0980 sensitized BRCA-competent TNBC cells to PARPi to induce an effective antitumor effect. This study demonstrates that an additional mechanism of action of GDC-0980 is the inhibition of the PI3K pathway–dependent DNA damage response, which is augmented by PARP inhibition owing to an inability to respond to additional DNA damage induced by carboplatin. The latter provides additional support that PI3K and mTOR regulate DNA damage responses both *in vitro* and *in vivo* and provides a strong mechanistic rationale for the combination of the PI3K-mTOR pathway inhibitors with PARPi in TNBC that are BRCA proficient (a BC subtype in which PARPi are not active).

Materials and Methods

Cell Culture, Reagents, and Antibodies

TNBC cell lines (HCC70, HCC1143, HCC1937, MDA-MB231, MDA468, and BT20) were obtained from American Type Culture Collection (ATCC, Manassas, VA) and cultured according to standard protocols. Antibodies against $pAKT^{S473}$, $pAKT^{T308}$, AKT,

pS6RP$^{S235-236}$, S6RP, p4EBP1$^{T37/46}$, 4EBP1, pERK$^{T202/Y204}$, ERK, cleaved PARP, a pro-apoptotic BH3-only of Bcl-2 family (BIM), and cleaved caspases 3 and 9 (Cell Signaling Technology, Danvers, MA), poly ADP-ribose (PAR) and PARP (Trevigen, Gaithersburg, MD), and pγH2AX^{S139} (Novus Biologicals, Littleton, CO) were used for the study. GDC-0980 and ABT888 were kindly supplied by Genentech, Inc (South San Francisco, CA) and National Cancer Institute (NCI, Bethesda, MD), respectively. *In vivo* studies were carried out using ABT888 purchased from ChemieTek (Indianapolis, IN).

Biochemical Analysis

We tested the effects of ABT888 plus carboplatin and GDC-0980 (alone and in combination) on a panel of five to seven BRCA–wild-type and BRCA-mutant TNBC cell lines. Normalized lysates (20-40 μg protein) were resolved by 10% sodium dodecyl sulfate–polyacrylamide gel electrophoresis for Western blot [28,29]. Doses of GDC-0980 (50 and 200 nM) and ABT888 plus carboplatin (2.5 and 10 μM) were used for the *in vitro* study.

Cell Cycle Analyses and Apoptosis

Cells were trypsinized, fixed, and permeabilized in cold 70% ethanol and then washed with RPMI (phenol red free with 1% FBS) and stained with 15 mg/ml propidium iodide (Sigma, St Louis, MO) plus 10 mg/ml RNaseA (Sigma) before analysis by flow cytometry (Accuri C6). To detect apoptosis, cells were resuspended in phosphate-buffered saline (PBS) containing 4 mM $CaCl_2$, 3% annexin V–phycoerythrin (PE; BD Pharmingen, San Jose, CA), and 3% 7AAD. Cells were analyzed by flow cytometry (Accuri C6).

Live/Dead Cell Assay and Immunofluorescence

We performed a fluorescence-based assay of live/dead cells using fluorescence kit from Invitrogen (Molecular Probes, Grand Island, NY) according to the manufacturer's protocol. In short, treated cells grown in 24-well plates were washed with PBS and incubated with a 0.5 μM Eth-D-1 and 0.5 μM calcein AM solution in PBS for 30 minutes at room temperature. Pictures were taken using an Olympus DP72 digital camera. Confocal microscopy (Nikon A1 TIRF Confocal; Nikon Instruments Inc, Melville, NY) was performed following immunofluorescence (IF) staining [28] for cleaved caspase 3 (Alexa Fluor 488), Ki67 (Alexa Fluor 647), and pγH2AX^{S139} (Alexa Fluor 488).

Clonogenic Growth Assay

Three-dimensional (3D) "ON-TOP" colony assay for anchorage-dependent clonogenic growth was standardized with little modificationfrom Lee et al. [30]. Pictures of the live colonies were taken using an Olympus DP72 digital camera. Soft agar assay for anchorage-independent clonogenic growth was performed using cells embedded in 0.4% low melt agar. Medium containing the drug treatment was layered on top and changed every 5 to 7 days. Live colonies (14 days) of cells were counted using an automated gel counter (Oxford Optronix; Oxfordshire, United Kingdom).

Xenograft Study and Pharmacodynamic Marker Analysis

In vivo efficacy of the drug combination was evaluated in athymic mice bearing established xenograft tumors following Institutional Animal Care and Use Committee (IACUC) guidelines. Cells (5×10^6 MDA-MB231 cells; 2×10^6 MDA-MB468 cells) were suspended in matrigel (50:50) and injected subcutaneously into the flank of immunocompromised female nude (nu/nu) mice, which were obtained from Taconic Farms, Inc (Germantown, NY). Our pilot *in vivo* studies test the effect of tumor on the overall health of the tumor-bearing mice to comply with the National Institutes of Health (NIH) and our institutional guidelines. The study showed that the tumors developed from the MDA-MB468 cell lines have an inherent tendency to have central necrotic areas especially when they tend to grow larger than 500 to 750 mm^3 in volume. Our experience from previous studies also show that it is because of the inherent nature of these PTEN-null MDA-MB468 cell lines that tumors show central necrotic areas as the volume of the tumor increases over time. In contrast, although tumors from MDA-MB231 xenografts increase in volume more than tumors from MDA-MB468 at the end of comparable time period, they do not show any signs of central necrosis and mice remain in proper health and ethical conditions for drug treatment. Considering the high burden of necrotic tumors in animals of control groups in MDA-MB468 model, we followed the advice of our institutional veterinarian to have 1) an alternate day schedule of drug administration for GDC-0980 and 2) halved the dose of ABT888 for the group of animals bearing MDA-MB468 xenograft tumors (to maintain healthy body weights and comply with ethical guidelines). Thus, to compare the effect the same drug combinations between MDA-MB468 xenograft tumors and MDA-MB231 xenograft tumors, we kept both the "starting tumor volume" and the "total days of drug treatment" constant, while we altered the drug schedule in MDA-MB468 xenograft tumor–bearing animals.

After injection of tumor cells, tumors were monitored until they reached mean tumor volumes of 150 to 300 mm^3 and were distributed randomly into groups of 8 to 10 animals per group [31]. GDC-0980 and GDC-0941 were formulated in 0.5% methyl cellulose/0.2% Tween-80 and administered (10 mg/kg in 100 μl) through oral gavage. ABT888 was administered orally. Carboplatin (Sanford Hospital Pharmacy, Sioux Falls, SD) was reconstituted and diluted in saline and dosed intravenously (i.v.) once on the first day of the treatment cycle. Tumor volumes were determined by digital calipers using the formula $(L \times W \times W)/2$ and expressed as mean relative tumor volume (mm^3). Tumor sizes and body weights were recorded twice weekly over the course of the study. Mice with tumor volumes >2000 mm^3 or with losses in body weight 20% or more from their weight at the start of treatment were killed per institutional IACUC guidelines. For the pharmacodynamic (PD) studies, tumors were analyzed for the markers shown at the end of the treatment period. For marker analysis, immunohistochemistry (IHC) was performed on the paraffin-embedded tumor tissue sections using Ki67, CD31, phosphorylated vascular endothelial growth factor receptor (pVEGFR), cleaved caspase 3, phospho-S6RP, and phospho-4EBP1 antibodies.

Statistical Analysis

All *in vitro* experiments were performed independently at least three times in triplicates. Statistical analyses were carried out using Microsoft Excel software. All numerical data are expressed as means ± SD between triplicate experiments. Significant differences were analyzed using Student's *t* test and two-tailed distribution. Data were considered to be statistically significant if $P < .001$. Student's *t* test is used to evaluate differences observed between treated groups and vehicle-treated controls. For *in vivo* studies, the overall *P* value for testing for differences between two groups is <.05.

Results

Dual Inhibition of PI3K and mTOR by GDC-0980 Alone Changed the State of the Repair of DNA Damage in BRCA-Competent TNBC Cells

Because PI3K signaling has been known to maintain HR steady state [15] and inhibition of mTOR 1) suppresses HR and NHEJ and 2) fails to recruit BRCA1 and RAD51 to DNA repair foci, an essential step for HR [32], we investigated whether dual inhibition of PI3K and mTOR would increase DNA damage in BRCA-proficient TNBC cells including MDA-MB231, MDA-MB468, HCC70, and BT20. We observed that GDC-0980 alone induced PAR-rylation in TNBC cells. In PTEN-null MDA-MB468 cells, 200 nM of the drug increased PAR slightly as early as 3 hours after treatment (Figure 1*A*, *upper panel*), while PAR levels were significantly high at both doses of GDC-0980 (50 and 200 nM) at 24 and 72 hours. In contrast, increases in PAR levels in RAS/RAF-mutated MDA-MB231 cells were modest only around 72 hours (Figure 1*A*, *lower panel*). Interestingly, increase in PAR levels coincided with a concomitant increase of phosphorylated histone 2AX (pγH2AX^{S139}), a DSB-related biomarker [33], levels in a dose-dependent, time-dependent, and cell-specific manner (Figure 1*B*). Thus, dual inhibition of PI3K and mTOR resulted in an accumulation of pγH2AX^{S139}, a protein that is localized to the damaged DNA [34] (to recruit effectors of DDR to these sites), which coincided with the gain of accumulated product/marker of PARP enzyme activation, PAR [35]. Levels of PAR, PARP, and pγH2AX^{S139} and the ratios of PAR/PARP as well as PAR/pγH2AX^{S139} in MDA-MB468 (Figure 1, *C* and *D*) and MDA-MB231 (Figures W1–W4) were semi-quantified from the density of bands using ImageJ. IF localization of the focal accumulation of pγH2AX^{S139} in MDA-MB468 cells after 24 hours of GDC-0980 treatment showed a profound increase of pγH2AX^{S139} foci (marker for DSB; Figure 1*E* and Movies W1–W4). Ki67 IF decreased in MDA-MB468 cells after 24 hours of GDC-0980 treatment (Figure 1*F*). A similar increase in the levels of PAR and pγH2AX^{S139} were observed in HCC70 and BT20 cells following 24 and 72 hours of the treatment of two doses of GDC-0980 (Figure 1, *G* and *H*). Both the levels of PAR and the ratio of PAR/PARP were significantly higher than the untreated cells at both time points in HCC70 and BT20 cells (Figure 1*I*). A similar increase in the ratio of PAR/pγH2AX^{S139} was also observed in both the cell lines following the GDC-0980 treatment (Figure 1*J*). Interestingly, the substantial increase in PAR levels in *PIK3CA*-mutated BT20 cells at 72 hours was found to be dose dependent (Figure 1*G*, *right bottom panel*).

Dual Inhibition of PI3K and mTOR by GDC-0980 Enhanced the State of DNA Damage in the Presence of Carboplatin plus PARP Inhibitor ABT888 in BRCA-Competent TNBC Cells

Because of the inherent genomic instability in part owing to deficiency in DDR [36], TNBC has been reported to be particularly sensitive to chemotherapy. Because we observed that GDC-0980 alone can induce a substantial impairment of DDR in BRCA-competent cells, we hypothesized that addition of carboplatin would increase the load of DNA damage at a given time and this load of DNA damage would be enhanced in the presence of ABT888 that inhibits the capacity of a tumor cell to repair SSBs. In this situation, addition of a dual PI3K-mTOR inhibitor would be expected to induce apoptosis even in BRCA-competent cells. To test this hypothesis, we treated the cells with ABT888 plus carboplatin in combination with two doses of GDC-0980. GDC-0980 alone and in combination with ABT888 plus carboplatin enhanced DNA damage in TNBC cells (Figure 1), whereas ABT888 alone or in combination with GDC-0980 plus carboplatin decreased the ratio of PAR/PARP and PAR/pγH2AX^{S139} in TNBC cells (Figures 1, W2 and W4).

We observed that while ABT888 plus carboplatin abrogated PAR formation in both MDA-MB468 and MDA-MB231 cells, addition of GDC-0980 caused a robust increase in pγH2AX^{S139} levels compared to both controls, an effect more pronounced in MDA-MB468 cells (Figure 1) at all time points tested. As expected, treatment with ABT888 plus carboplatin blocked GDC-0980–induced PAR-rylation in both cell lines at all time points (comparable to ABT888 plus carboplatin treatment only; Figure 1). Yang et al. [37] reported that ABT888 hits its therapeutic target by significantly reducing PAR levels and the ratio of PAR to PARP-1 in human tumor cells as detected by IHC in tumors from a phase 0 trial conducted at the NCI. Similar to their study, we observed a reduction of PAR levels and the ratio of PAR to PARP-1 in both MDA-MB231 and MDA-MB468 cells. Although baseline PAR levels varied considerably between cell lines similar to that was observed by Yang et al., in MDA-MB468 cells, PAR levels

Figure 1. Effect of GDC-0980 alone and in combination with ABT888 plus carboplatin on DNA repair (PARP-mediated PAR formation), DNA damage (pγH2AX^{S139}), ratio of PAR/PARP, ratio of PAR/pγH2AX^{S139}, and IF distribution of pγH2AX^{S139} in four BRCA-competent TNBC cell lines. Expression of PAR (A) and pγH2AX^{S139} (B) by Western blot analysis of lysates from MDA-MB468 and MDA-MB231 treated with two doses of GDC-0980 (50 and 200 nM) alone or in combination with ABT888 (10 μM) plus carboplatin (10 μM) for different time points. β-Actin was used as a loading control. The semi-quantification of expression levels (of the ImageJ intensities of protein expression) of cellular PAR (upper panel), total PARP (middle panel), and ratio of PAR to total PARP (lower panel) (C), as well as pγH2AX^{S139} levels (upper panel) and ratio of PAR to pγH2AX^{S139} (lower panel) (D) in MDA-MB468 cells before and after treatments at different time points (3, 24, and 72 hours in successive darker shades) was shown as bar diagrams. Projection of 3D reconstituted *Z*-sections of confocal images (Nikon A1 TIRF Confocal; Nikon Instruments Inc) shows pγH2AX^{S139} IF in MDA-MB468 cells treated with 200 nM GDC-0980 for 24 hours (E). A merged image of pγH2AX^{S139} IF shows nuclear pγH2AX^{S139} foci (fluorescein isothiocyanate; green) with cytoplasmic filamentous actin (Phalloidin 555; red). Merged images of nuclear Ki67 (Alexa Fluor 647; visualized as pink pseudocolor) IF in MDA-MB468 cells show a decrease in staining after 24 hours of GDC-0980 treatment (200 nM) (F). Expression of PAR (G) and pγH2AX^{S139} (H) by Western blot analysis of lysates from HCC70 and BT20 treated with two doses of GDC-0980 (50 and 200 nM) alone or in combination with ABT888 (10 μM) plus carboplatin (10 μM) for different time points. β-Actin was used as a loading control. The semi-quantification of expression levels (of the ImageJ intensities of protein expression) of cellular PAR (upper panel), total PARP (middle panel), and ratio of PAR to total PARP (lower panel) (I), as well as pγH2AX^{S139} levels (upper panel) and ratio of PAR to pγH2AX^{S139} (lower panel) (J) in HCC70 and BT20 cells before and after treatments at different time points (3 and 72 hours in successive darker shades) was shown as bar diagrams.

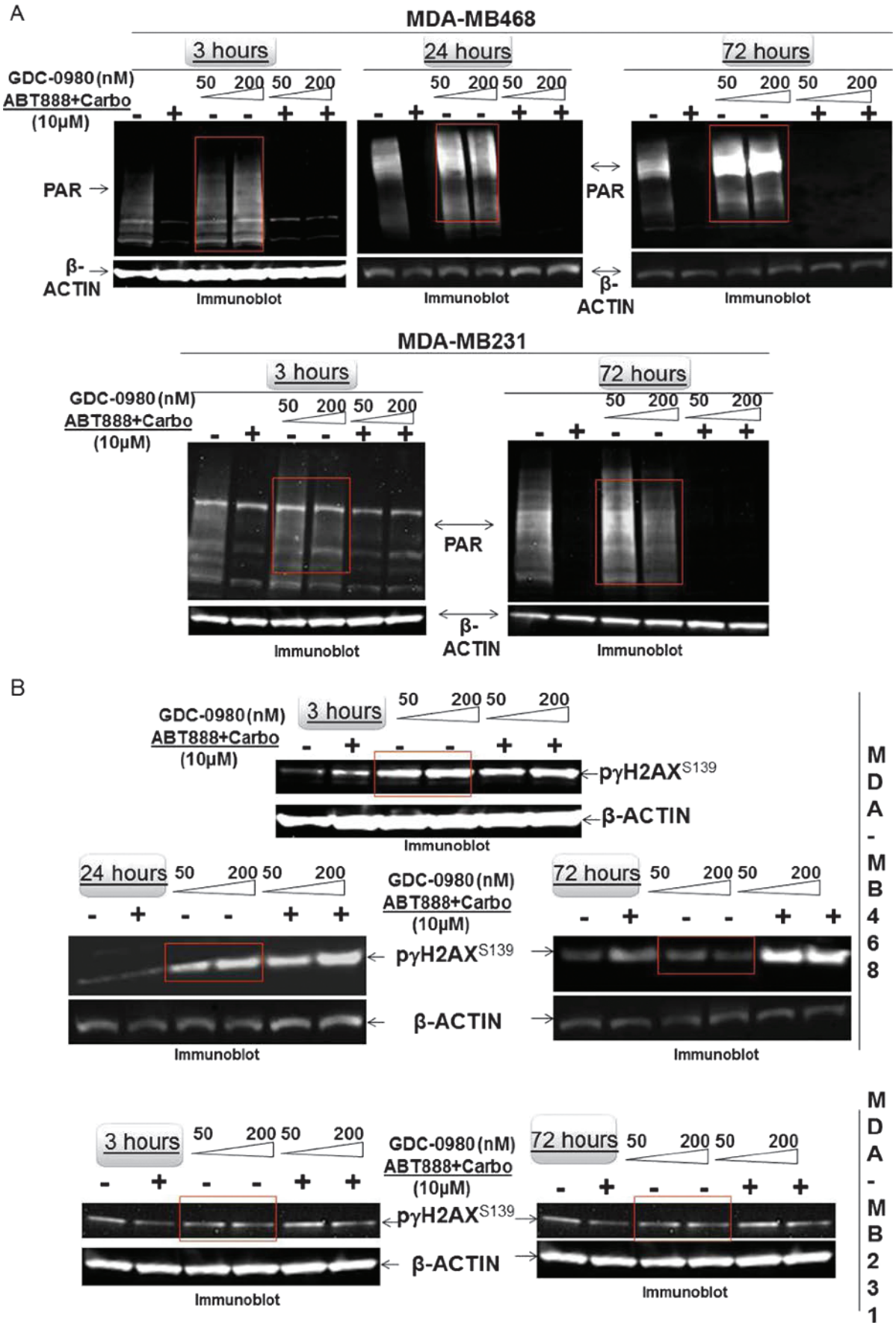
A
MDA-MB468
3 hours
24 hours
72 hours
GDC-0980(nM)
ABT888+Carbo
(10μM)
50 200 50 200
PAR
β-ACTIN
Immunoblot
MDA-MB231
B
pγH2AX S139
β-ACTIN
MDA-MB468
MDA-MB231

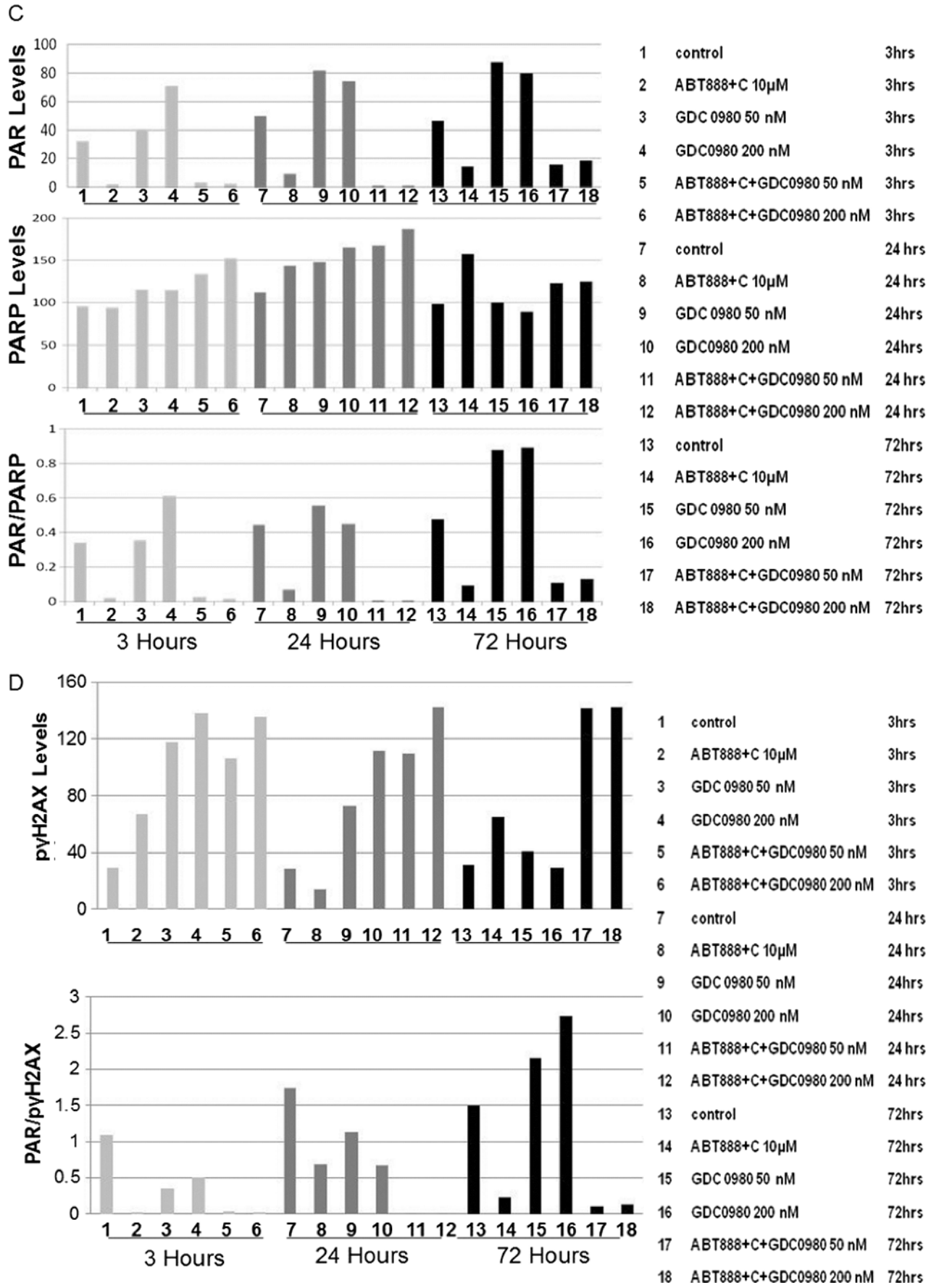

Figure 1. (*continued*).

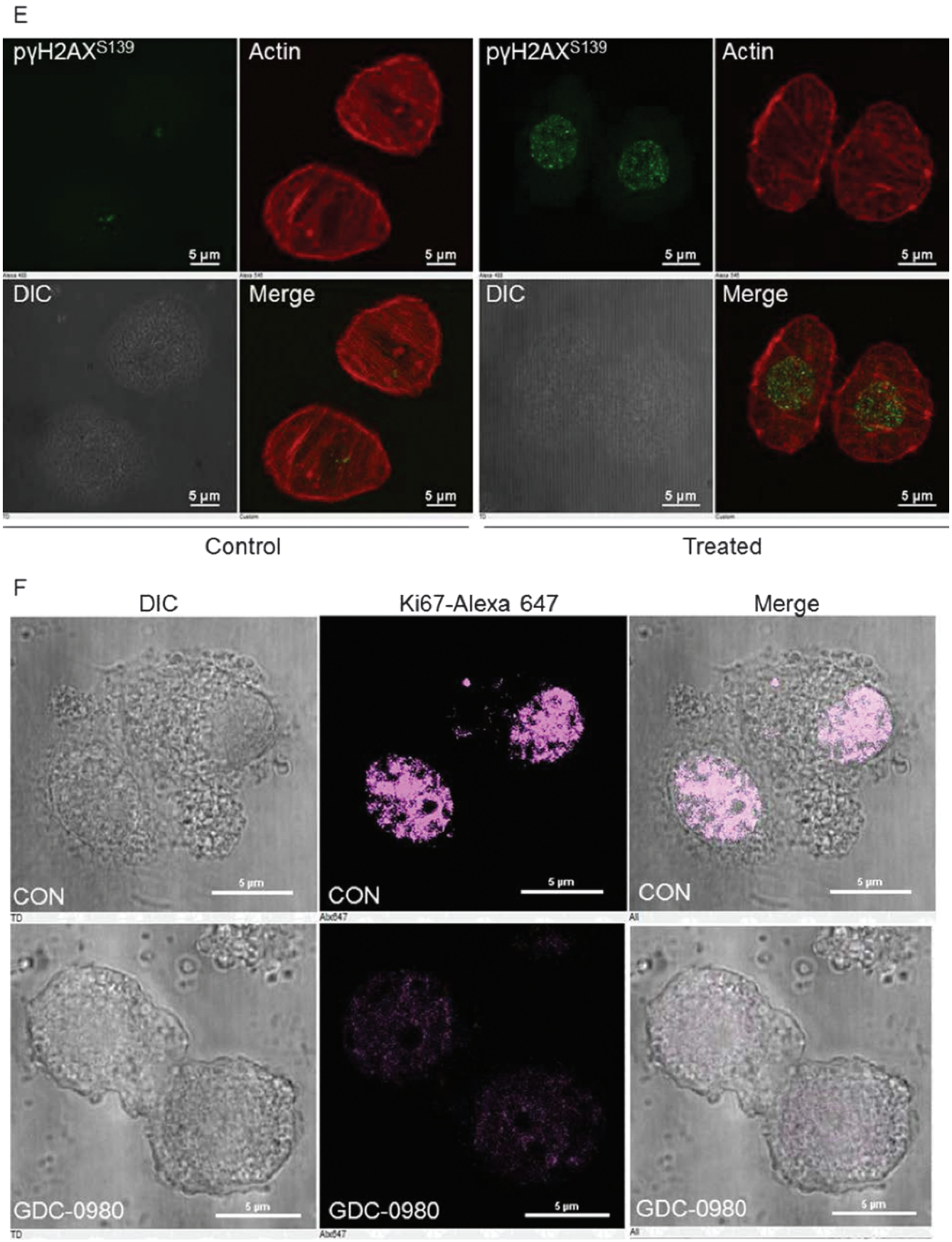

Figure 1. (*continued*).

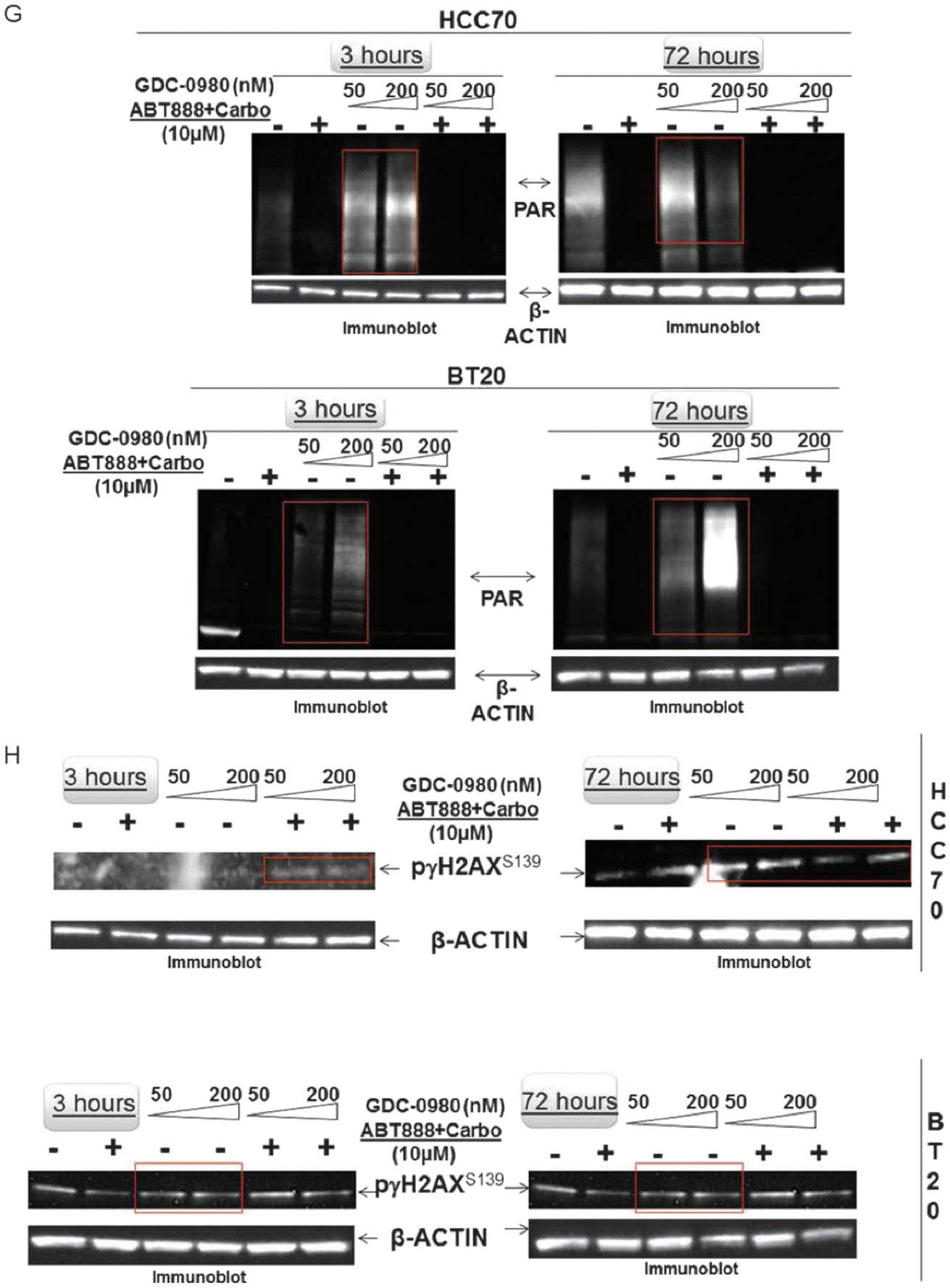

Figure 1. (*continued*).

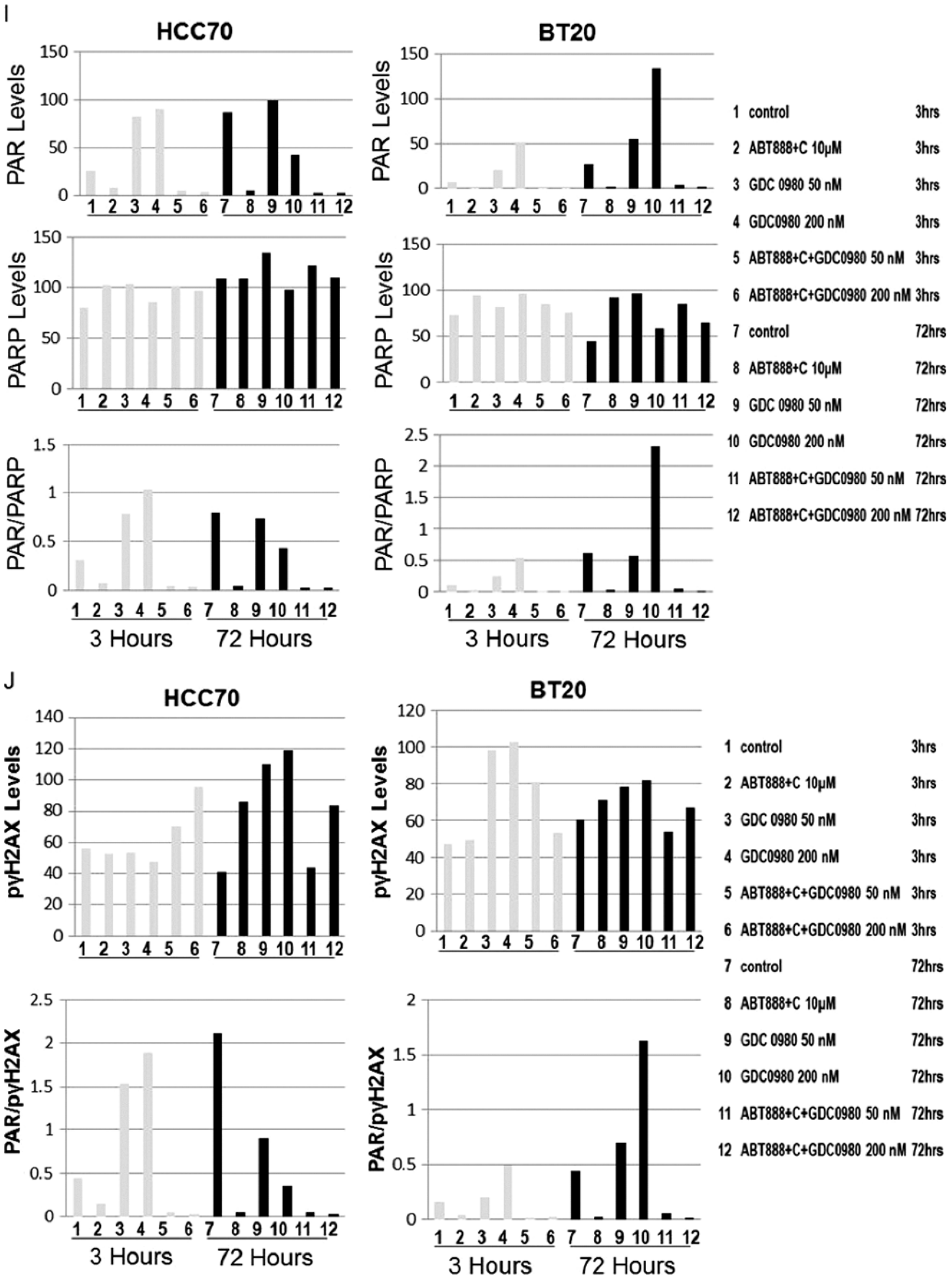

Figure 1. (*continued*).

and the ratio of PAR to PARP-1 were decreased from as early as 3 hours, whereas in MDA-MB231 cells, the decrease was most pronounced at 72 hours following the treatment with ABT888 alone or in combination with GDC-0980 (Figures 1 and W2).

Inhibition of PARP has been shown to increase pγH2AX foci formation, and this increase is thought to reflect the collapse of increased number of unresolved spontaneously formed SSBs (following PARP inhibition collapsing into DSBs at replication forks), which then are the major lesions triggering spontaneous HR [38]. Dual suppression of PI3K and mTOR by GDC-0980 enhanced the impairment of DDR in the presence of carboplatin plus ABT888 more than GDC-0980 alone or ABT888 plus carboplatin treatment. To substantiate the feasibility of detection of PAR polymer in the cells, we also determined pγH2AX^{S139} and expressed it as the ratio of PAR/pγH2AX^{S139}. Increased levels of pγH2AX^{S139} (more pronounced in MDA-MB468) with an abrogation of PAR (as shown by the decrease of PAR/pγH2AX^{S139} ratios) at all time points in MDA-MB468 and at 72 hours in MDA-MB231 cells following combination treatment demonstrated that inhibition of PARP had a significant contribution to the induction of DSB (pγH2AX^{S139} levels; Figures W2–W4).

To test the effectiveness of the treatment of GDC-0980 either alone or in combination with ABT888 plus carboplatin, we have included two BRCA-competent cell lines in which PI3K pathway activation has been reported to occur through two different ways, e.g., PTEN nullness (HCC70) and activating mutation of *PIK3CA* (BT20) [17]. The data demonstrated that the pattern of changes in the levels of PAR and pγH2AX^{S139} as well as the ratios of PAR/PARP and PAR/pγH2AX^{S139} in HCC70 and BT20 TNBC cell lines following the combination treatment at 24 and 72 hours was similar to that observed in MDA-MB231 and MDA-MB468 cells (Figure 1, *G–J*).

GDC-0980 Alone and in Combination with ABT888 plus Carboplatin Inhibited Cellular Survival/Proliferative Signals and Increased Cellular Apoptotic Signals in BRCA-Competent TNBC Cells

The effect of GDC-0980 alone or in combination with ABT888 plus carboplatin inhibited cellular survival/proliferative signals in MDA-MB468 and MDA-MB231 cells (Figure 2). Treatment with GDC-0980 caused a dose-dependent inhibition of pAKT^{T308}, pAKT^{S473}, pP70S6K, and pS6RP$^{S235-236}$ in MDA-MB468 cells at 3 and 24 hours. Combination with ABT888 plus carboplatin inhibited pAKT^{T308} more than the pAKT^{S473}, an effect similar to GDC-0980 treatment alone along with the inhibition of pS6RP$^{S235-236}$ at 3 hours (Figure 2, *A* and *B*). In MDA-MB231 cells, both GDC-0980 alone and in combination with ABT888 plus carboplatin decreased levels of pAKT^{T308}, pAKT^{S473}, and pS6RP$^{S235-236}$ at 3 hours, whereas the decrease in levels of pAKT^{T308} and pS6RP$^{S235-236}$ was restored at 72 hours. GDC-0980 alone and in combination with ABT888 plus carboplatin initially decreased both levels of p4EBP1$^{T37/46}$ and pERK$^{T202/Y204}$ dose dependently at 3 hours; most of which were restored at 72 hours with the exception of p4EBP1$^{T37/46}$ for the combined treatment (Figure 2*C*). We observed that pERK$^{T202/Y204}$ levels were restored at 72 hours after initial decrease at 3 hours in MDA-MB231 cells (Figure 2). It is possible that the restored levels of pERK$^{T202/Y204}$ at 72 hours were responsible for restored levels of pS6RP$^{S235-236}$, p4EBP1$^{T37/46}$, and pAKT^{T308}. Half maximal inhibitory concentration (IC_{50}) of GDC-0980 is lower for PI3Kα than mTOR kinase, which may explain in part the differences in the downstream inhibition. A similar decrease in the levels of pAKT^{S473}, pAKT^{T308}, pS6RP$^{S235-236}$, and p4EBP1$^{T37/46}$ was observed in HCC70 and BT20 cells following the treatment of GDC-0980 alone or in combination with ABT888 plus carboplatin (Figure 2, *G* and *H*).

Treatment with GDC-0980 in combination with ABT888 plus carboplatin caused a significant increase of cleaved PARP in MDA-MB468 cells starting as early as 3 hours until 72 hours (Figure 2*D*). We also observed an increase in cleaved PARP following ABT888 plus carboplatin at 24 and 72 hours, which was absent in MDA-MB231 cells. In MDA-MB468 cells, there was a differential up-regulation of cleaved caspases 3 and 9 and BIM at 72 hours (Figure 2*E*). GDC-0980 in combination with ABT888 plus carboplatin induced cleaved PARP and increased the ratio of cleaved PARP/t-PARP (Figure 2*E*, *inset*), a cleavage product of activated (cleaved) caspase 3. As a consequence, we tested IF for cleaved caspase 3 in the more sensitive MDA-MB468 cells at the highest time point after drug treatment. Cytoplasmic IF for cleaved caspase 3 was significantly increased in MDA-MB468 cells at 72 hours of treatment with the combination of the drugs (Figure 2*F*). A similar increase in the levels of cleaved PARP as well as the ratio of cleaved PARP/total PARP was observed in both HCC70 and BT20 cells following the treatment of GDC-0980 alone or in combination with ABT888 plus carboplatin

Figure 2. Effect of GDC-0980 alone and in combination with ABT888 plus carboplatin on cellular survival/proliferative signals, apoptotic signals, and IF distribution of cleaved caspase 3 in four BRCA-competent TNBC cell lines. Expression of survival/proliferative (A–C) and apoptosis markers (D–F) by Western blot and IF from cells treated with two doses of GDC-0980 (50 and 200 nM) alone or in combination with ABT888 plus carboplatin for different time points using the indicated antibodies is presented. A comparison of the apoptosis markers expressed at 72 hours of treatment with drugs between MDA-MB468 and MDA-MB231 is shown in E. Inset showed changes in expression of PARP, cleaved PARP (red rectangle; in the same blot), and the ratio of cleaved PARP/t-PARP in MDA-MB468. β-Actin was used as a loading control. Cleaved caspase 3 expression in MDA-MB468 cells at 72 hours by IF (control and triple combination) is shown (F). Projection of 3D reconstituted *Z*-sections of confocal images (Nikon A1 TIRF Confocal; Nikon Instruments Inc) shows a merged image of cytoplasmic cleaved caspase 3 IF (fluorescein isothiocyanate–conjugated cleaved caspase 3; green) with filamentous actin (Phalloidin 555; red) and 4′,6-diamidino-2-phenylindole (DAPI; blue) in *XYZ* axes (as shown in the pictures) in control (0.6-μm step size, 6.0-μm depth) and ABT888 + carboplatin + GDC-0980–treated (0.6-μm step size, 5.4-μm depth) MDA-MB468 cells. Inset shows differential interference contrast microscopy (DIC) image of the individual cells. Expression of survival/proliferative (G and H) and apoptosis markers (I and J) by Western blot from HCC70 and BT20 cells treated with two doses of GDC-0980 (50 and 200 nM) alone or in combination with ABT888 plus carboplatin for two different time points (3 and 72 hours) using the indicated antibodies is presented. I and J showed changes in expression of cleaved PARP and cleaved caspase 3 (red rectangle; in the same blot) in HCC70 (I) and BT20 (J) cell lines. β-Actin was used as a loading control. Insets of I and J showed changes in expression of the ratio of cleaved PARP/t-PARP in HCC70 (I) and BT20 (J) cell lines. β-Actin was used as a loading control.

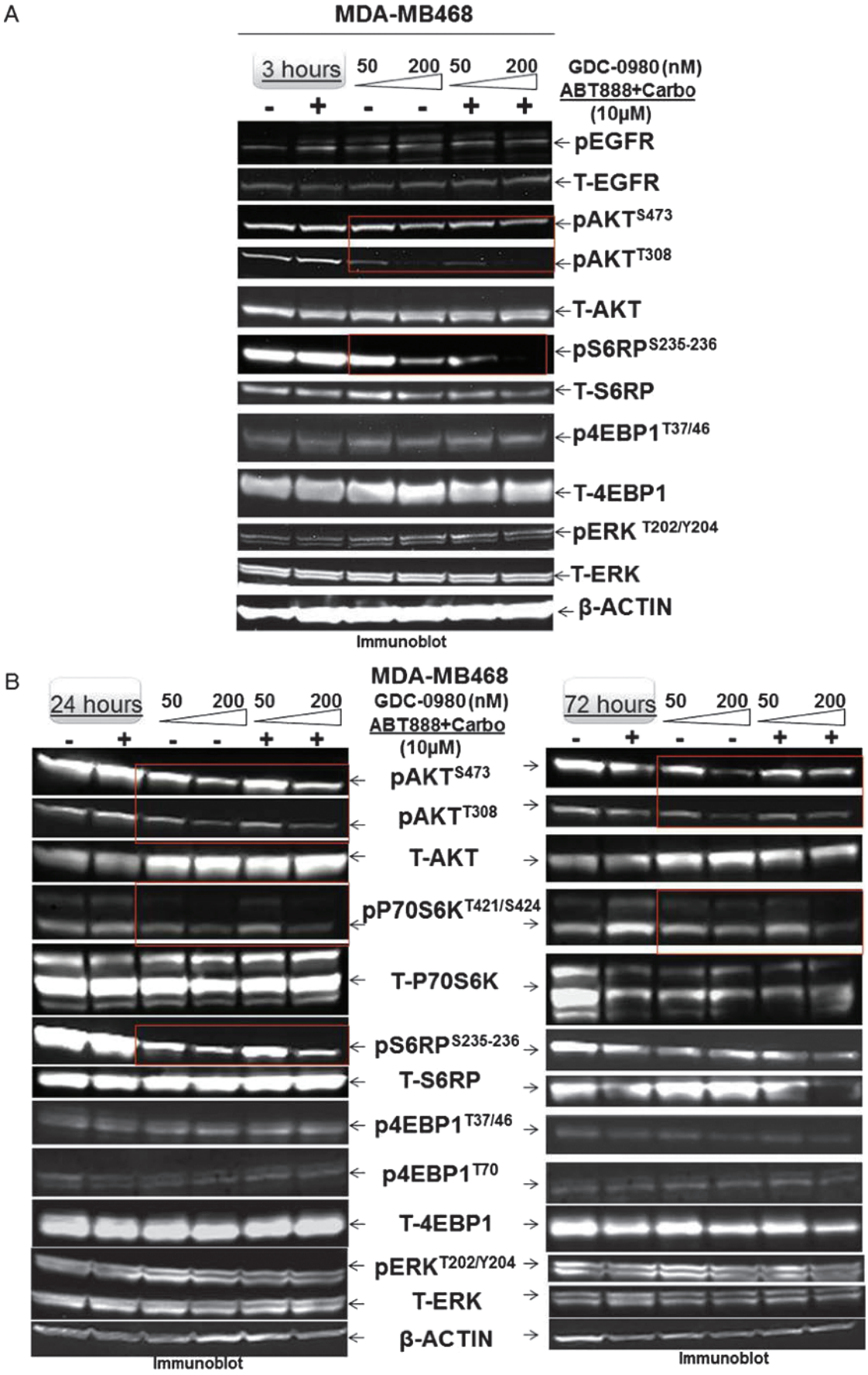
A
MDA-MB468
3 hours
50 200 50 200
GDC-0980 (nM)
ABT888+Carbo (10μM)
- + - - + +
pEGFR
T-EGFR
pAKT S473
pAKT T308
T-AKT
pS6RP S235-236
T-S6RP
p4EBP1 T37/46
T-4EBP1
pERK T202/Y204
T-ERK
β-ACTIN
Immunoblot
B
MDA-MB468
24 hours
72 hours
50 200 50 200
GDC-0980 (nM)
ABT888+Carbo (10μM)
- + - - + +
pAKT S473
pAKT T308
T-AKT
pP70S6K T421/S424
T-P70S6K
pS6RP S235-236
T-S6RP
p4EBP1 T37/46
p4EBP1 T70
T-4EBP1
pERK T202/Y204
T-ERK
β-ACTIN
Immunoblot
Immunoblot

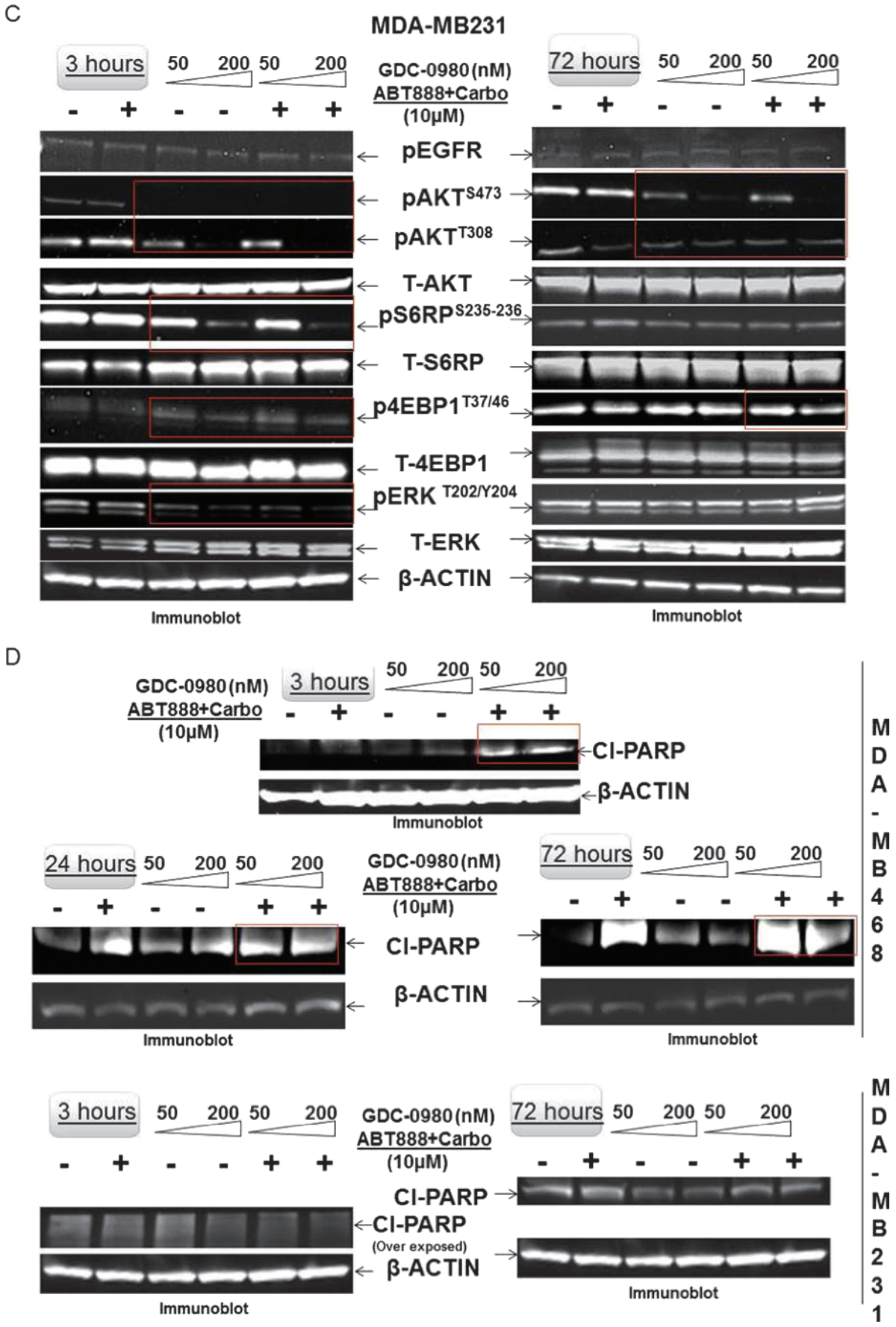

Figure 2. (*continued*).

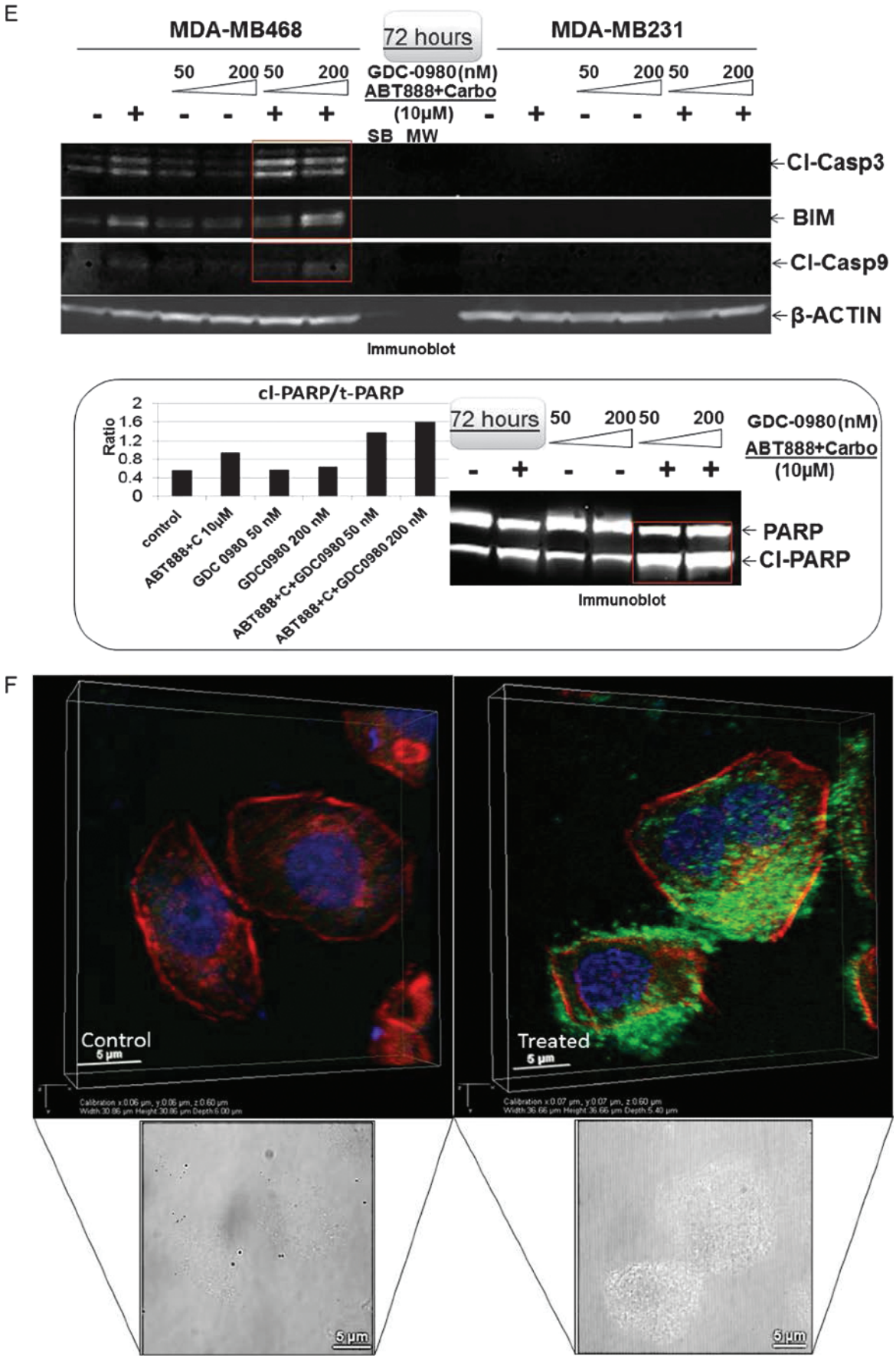

Figure 2. (*continued*).

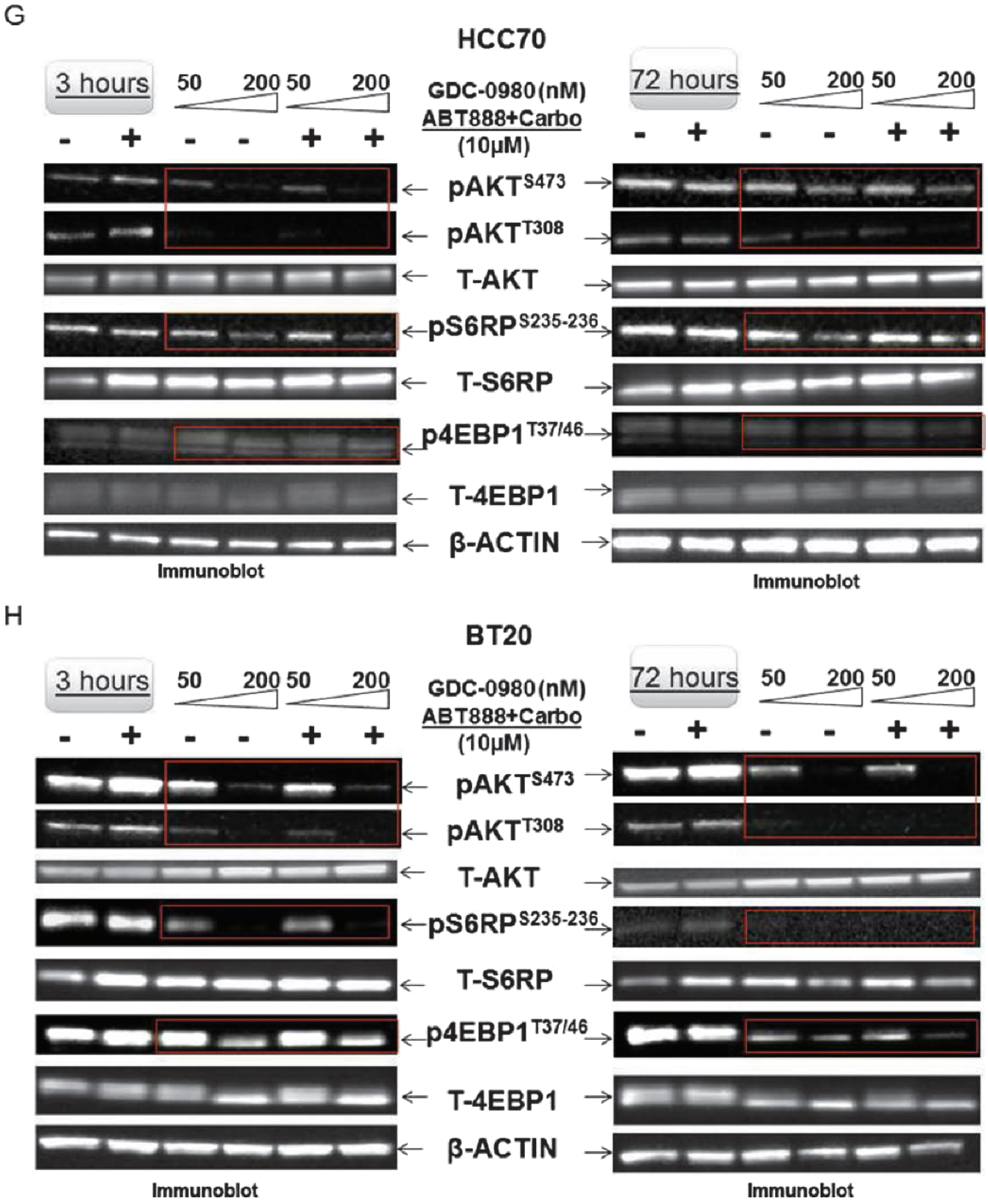

Figure 2. (*continued*).

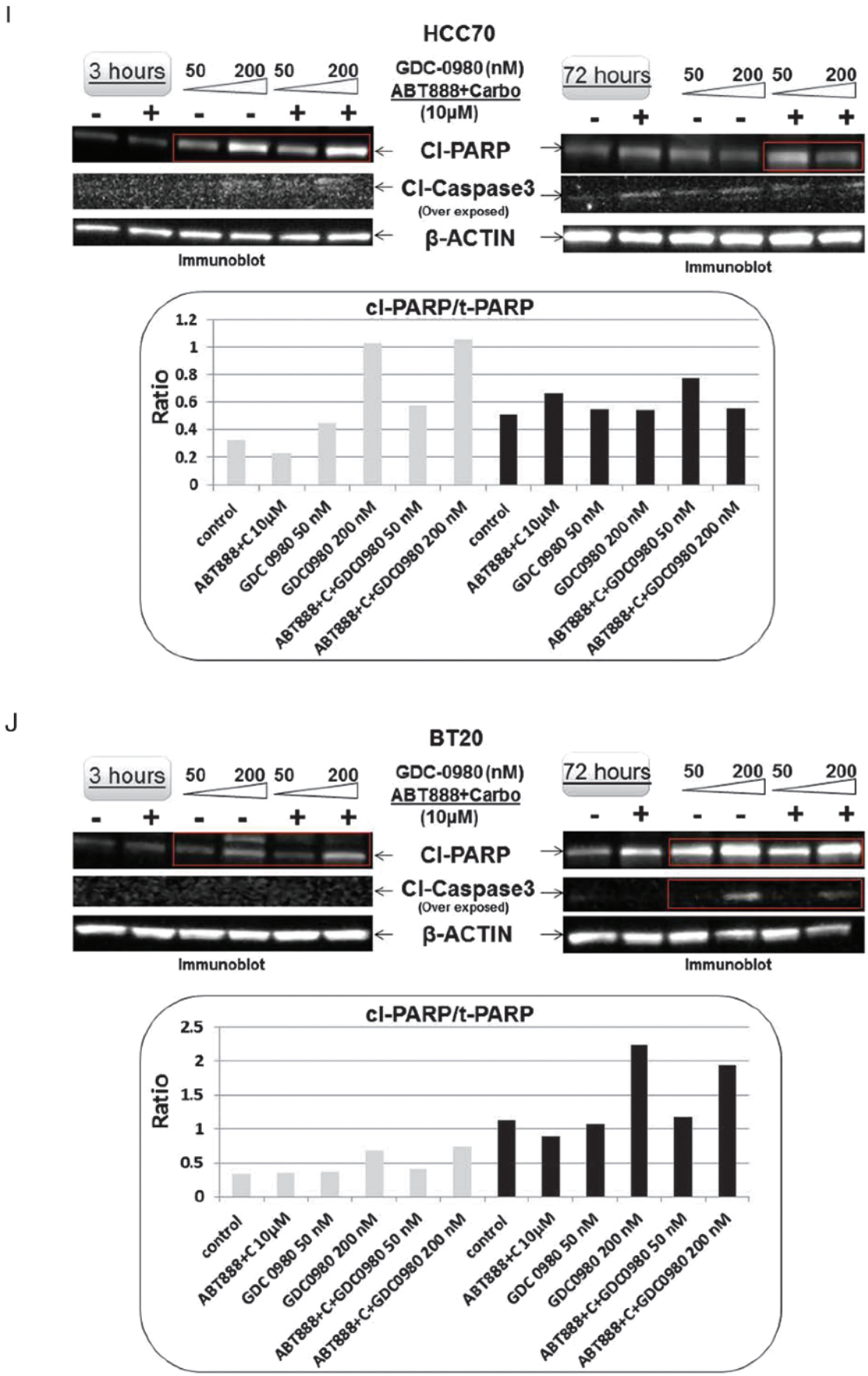

Figure 2. (*continued*).

(Figure 2, *I* and *J*). However, the increases in the cleaved caspase 3 levels were more prominent at later time point (72 hours) in both the cell lines (Figure 2, *I* and *J*, *middle panel*).

GDC-0980 Alone and in Combination with ABT888 plus Carboplatin Inhibited Cell Cycle Progression, Increased Apoptosis, and Decreased Live/Dead Cell Ratios in BRCA-Competent TNBC Cells

For the cell cycle progression study, TNBC cell lines in which the PI3K/AKT pathway is activated in the absence of PTEN (MDA-MB468) or an activating mutation of PI3K (BT20) and in which the RAS/mitogen-activated protein kinases (MAPK) pathway is activated (MDA-MB231) were used. Flow cytometric analyses revealed that although MDA-MB231 cells exhibited certain resistant characteristics following treatment with ABT888 plus carboplatin, the G_2 phase response of the cells to GDC-0980 was comparable to MDA-MB468. Both cell lines showed an increase in annexin V positivity following GDC-0980 alone or in combination with ABT888 plus carboplatin at 48 hours. A dose-dependent increase in the G_1 phase population was observed following GDC-0980 in all cell lines tested (Figures 3, *A* and *B*, and W5). This trend was preserved when combined with ABT888 plus carboplatin. Treatment of cells with ABT888 plus carboplatin decreased the G_2 phase in MDA-MB468 cells compared to the other two cell lines. However, the decrease of the G_2 phase was observed following GDC-0980 in all three cell lines irrespective of their mutation status. A dose-dependent increase in the sub-G_1 (G_0) peak following GDC-0980 was also observed in all cells by 24 hours of treatment, which persisted for 72 hours (data not shown). Because we observed an increase in markers of apoptosis (cleaved PARP, cleaved caspases 3 and 9, and BIM) following treatment, we tested the early event of apoptosis at 48 hours. Annexin V/7AAD staining indicated that GDC-0980 alone and in combination with ABT888 plus carboplatin increased early events of apoptosis in TNBC cells in a dose-dependent manner in both MDA-MB468 and MDA-MB231 cells (Figure 3*C*). In agreement with these data, the combination of GDC-0980 with ABT888 plus carboplatin decreased the live/dead cell ratios more profoundly in MDA-MB468 cells (Figure 3*D*) compared to MDA-MB231 cells (data not shown). We have also tested the effects of combination of GDC-0941 with ABT888 plus carboplatin *in vitro* in the more sensitive and PTEN-null MDA-MB468 cell line. GDC-0941 alone or in combination with ABT888 plus carboplatin demonstrated 1) a trend in the increase in the G_1 phase and a decrease in the G_2 phase of cell cycle at 24 hours (Figure 3*E*), 2) an increase in the annexin V positivity of cells at 48 hours (Figure 3*F*), and 3) a decrease in 2D colony formation on soft agar (Figure 3*G*).

GDC-0980 Alone and in Combination with ABT888 plus Carboplatin Attenuated an Anchorage-Dependent and Anchorage-Independent Clonogenic 3D Growth in BRCA-Competent TNBC Cells

Since we observed a decrease in proliferative signal and an increase in proapoptotic signal as well as increase in apoptosis following drug treatment, we tested the effect of the drug combination on clonogenic growth of these cells. GDC-0980 dose dependently blocked colony formation in 3D ON-TOP assay (Figure 4, *A* and *B*) as well as in soft agar assay (Figure 4*C*). Although a combination of GDC-0980 with ABT888 plus carboplatin had a synergistic inhibitory effect on colony formation by both soft agar assay and 3D ON-TOP assay in MDA-MB468 and MDA-MB231 cells (Figure 4*C*), we observed that consistent with our previous results, the highest dose of GDC-0980 (200 nM) completely blocked colony formation synergistically in combination with ABT888 plus carboplatin in MDA-MB468 cells. Interestingly, the lower dose (50 nM) of GDC-980 in the MDA-MB468 soft agar assay also significantly blocked colony formation synergistically in combination with ABT888 plus carboplatin. However, the highest dose of GDC-0980 (200 nM) in combination with ABT888 plus carboplatin failed to bring a comparable level of inhibition of the formation of colonies in MDA-MB231 cells when compared to GDC-0980 alone.

GDC-0980 Alone and in Combination with ABT888 plus Carboplatin Is Efficacious in BRCA-Competent MDA-MB468 and MDA-MB231 Xenograft Models

The *in vitro* sensitivity profile of GDC-0980 alone and in combination with ABT888 plus carboplatin was recapitulated *in vivo* in MDA-MB468 (Figure 5) and MDA-MB231 xenograft models (Figure 6), and the combination was efficacious in both the BRCA-competent TNBC xenograft models tested. We also confirmed the efficacy of combination in a more clinically relevant disease model of TNBC, MDA-MB468 that does not expresses PTEN protein. A combination of ABT888 plus carboplatin was typically efficacious

Figure 3. Effect of GDC-0980 and GDC-0941 alone and in combination with ABT888 plus carboplatin on cell cycle progression, apoptosis, and live/dead cells in BRCA-competent TNBC cell lines. Effect of two doses of GDC-0980 (50 and 200 nM) alone or in combination with ABT888 (2.5 μM) plus carboplatin (2.5 μM) on cell cycle distribution in MDA-MB468 (A) and MDA-MB231 (B). Cells were treated as indicated for 24 hours. Cells were released and ethanol fixed before staining with propidium iodide for analysis by flow cytometry. (C) Effect of GDC-0980 (50 and 200 nM) alone or in combination with ABT888 plus carboplatin on apoptotic (early) response analyzed by annexin V/7AAD staining in MDA-MB468 and MDA-MB231. Cells were treated for 48 hours, released, rinsed, and placed in annexin V binding buffer. Cells were labeled with annexin V–PE and 7AAD for analysis. Error bars represent SEM from triplicates. (D) Effect of GDC-0980 in combination with ABT888 plus carboplatin on live (green)/dead (red) cells in MDA-MB468 cells was shown. The merged image is shown to depict the live/dead cells. The dead cells were separately shown in the right panel. Effects of GDC-0941 (500 and 1000 nM) alone or in combination with ABT888 (2.5 μM) plus carboplatin (2.5 μM) on cell cycle distribution (E) and on apoptotic (early) response analyzed by annexin V/7AAD staining (F) in MDA-MB468. Cells were treated as indicated for 24 hours for the cell cycle analyses and 48 hours for annexin V/7AAD staining. Effect of GDC-0941 alone and in combination with ABT888 plus carboplatin on 2D clonogenic growth under anchorage-independent conditions in MDA-MB468 TNBC cells is presented (G). MDA-MB468 cells were plated under anchorage-independent conditions (soft agar assay) for 10 to 15 days and pictures of live colonies were taken (Olympus DP32; original magnification, $\times$4). Cell colonies were counted using an automatic gel counter. Data represent bar diagrams of the number of colonies (percentage of controls) in the respective groups of three independently performed experiments.

in the MDA-MB468 xenograft model in which the PI3K-mTOR pathway was activated because of genetic alterations associated to the loss of PTEN protein. In this model, delay in tumor growth (stasis) was achieved at the 10 mg/kg dose administrated every other day compared to the daily dose of GDC-0980 in the MDA-MB231 model. In the MDA-MB468 model, a comparable inhibition of tumor growth was achieved with 12.5 mg/kg ABT888 (twice a day, for 5 days) compared to 25 mg/kg ABT888 in the MDA-MB231 model. In contrast to the MDA-MB468 model, MDA-MB231, the TNBC cell line/xenograft model that harbors mutations in KRAS or BRAF,

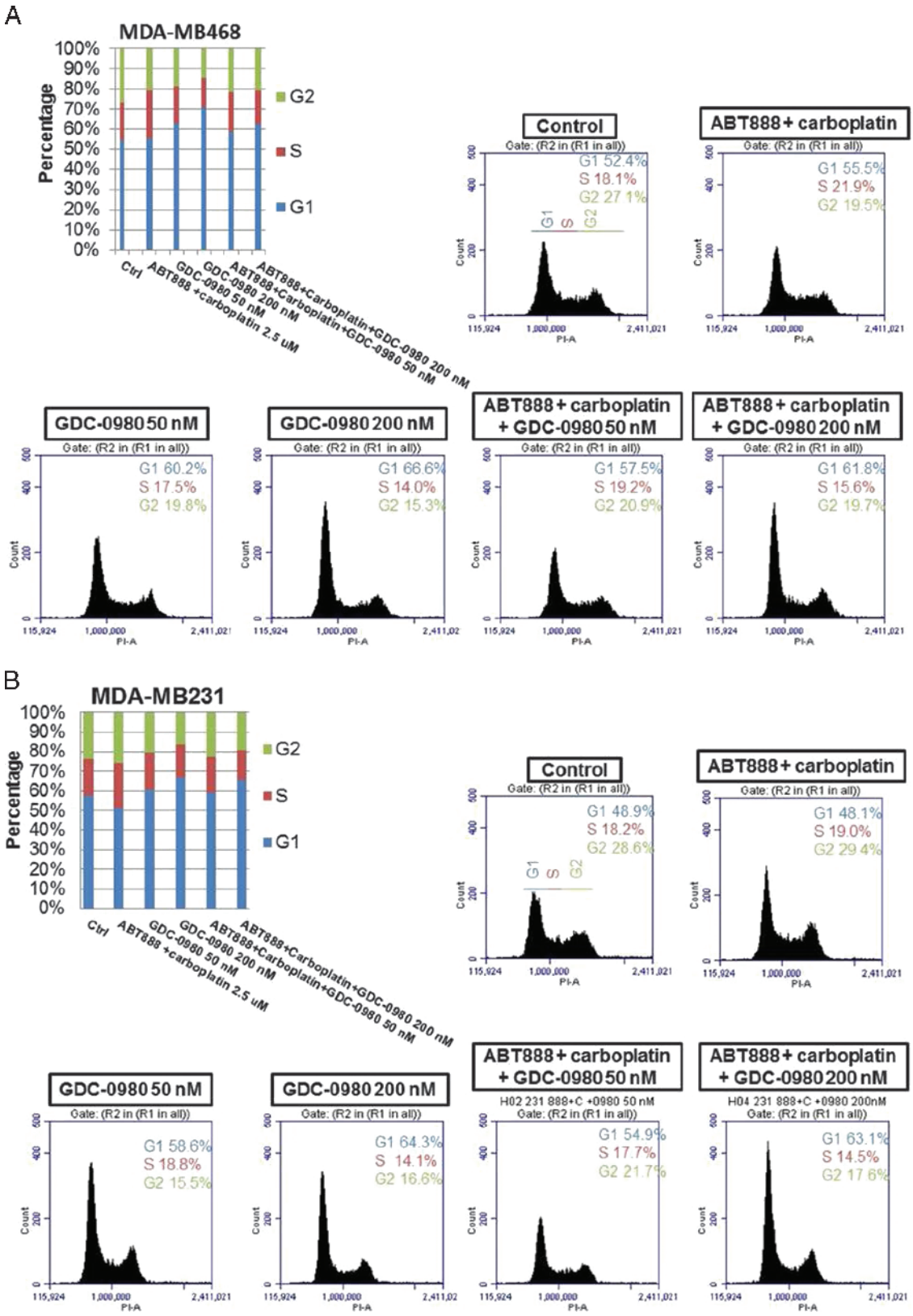

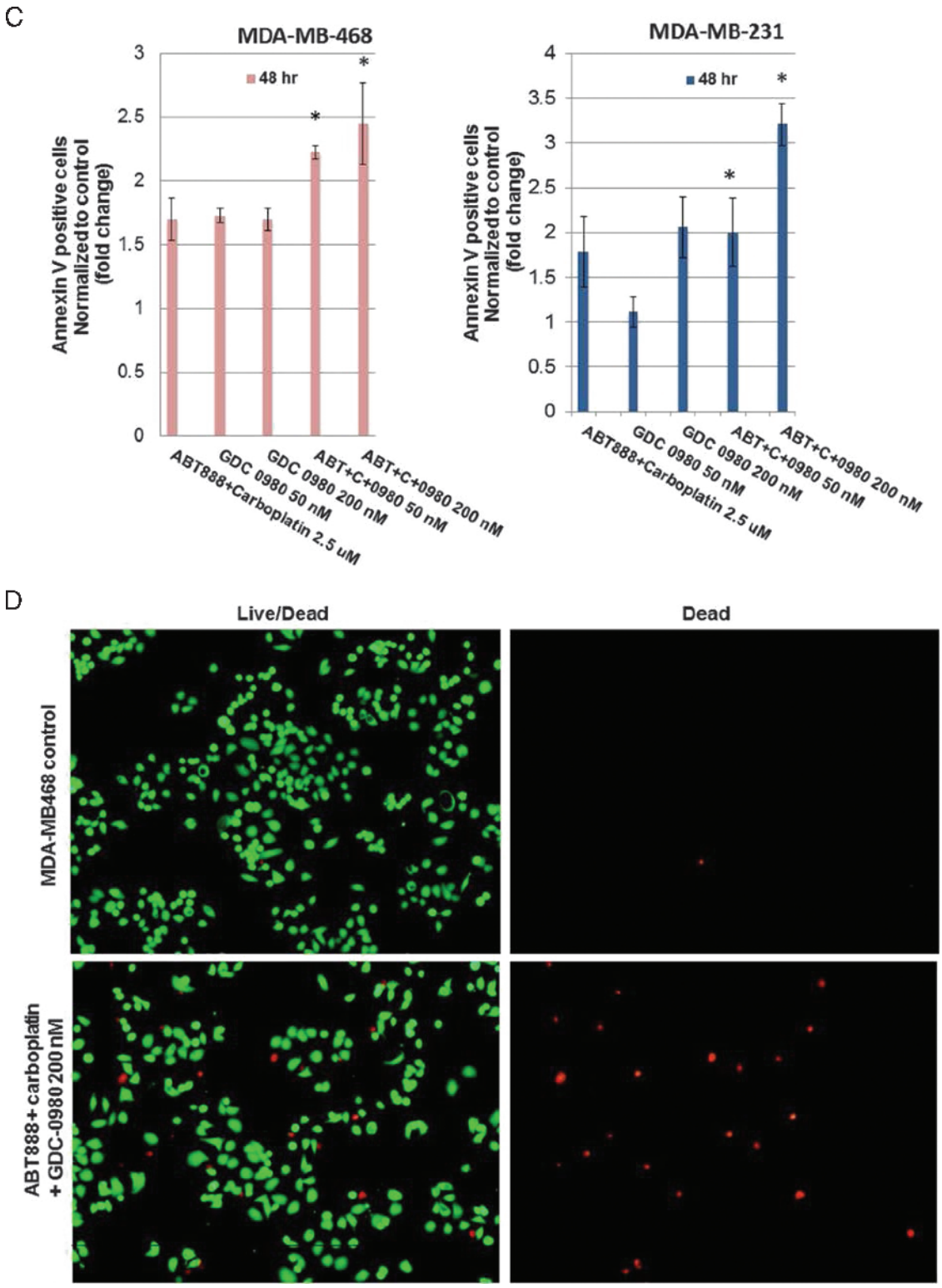

Figure 3. (*continued*).

was less sensitive to GDC-0980 alone (nonsignificant decrease of the established tumor) and in combination with ABT888 plus carboplatin. However, a significant reduction of tumor growth was achieved following the combination of ABT888 plus carboplatin and GDC-0980 in this xenograft with a higher dose of ABT888 and a more frequent dosing of GDC-0980 compared to the combination regimen used in the MDA-MB468 model. Single agent treatment of GDC-0980 was well tolerated with less than 10% body weight loss observed compared with vehicle controls in both models (Figures 5*A* and 6*A*). In the MDA-MB468 model, while carboplatin alone or GDC-0980 alone showed a trend (nonsignificant) of decrease in tumor growth, ABT888 plus carboplatin combination was efficacious. When tested *in vivo*, GDC-0980 in combination with ABT888 plus carboplatin induced tumor stasis in the MDA-MB468 xenograft

model, at doses where each single agent was ineffective. The result of our study showed that although comparable inhibitions of tumor growths were observed in both models using the same drug combinations, the efficacy of the combination was higher in MDA-MB468. This is because of the fact that the drug schedule for GDC-0980 was more frequent (daily injections) as well as the drug dose for ABT888 was double (25 mg/kg) in the MDA-MB231 model compared to an alternate day of GDC-0980 injections and 12.5 mg/kg injection of ABT888 in the MDA-MB468 model. On the contrary, we have observed that pan-PI3K inhibitor GDC-0941 in combination with ABT888 plus carboplatin failed to inhibit the growth of the established tumors in the MDA-MB231 xenograft model when compared with GDC-0980 (Figure 6*F*).

To further investigate the mechanism of action of GDC-0980 alone or its combination with ABT888 plus carboplatin on tumor growth inhibition, expression levels of proliferative marker (Ki67),

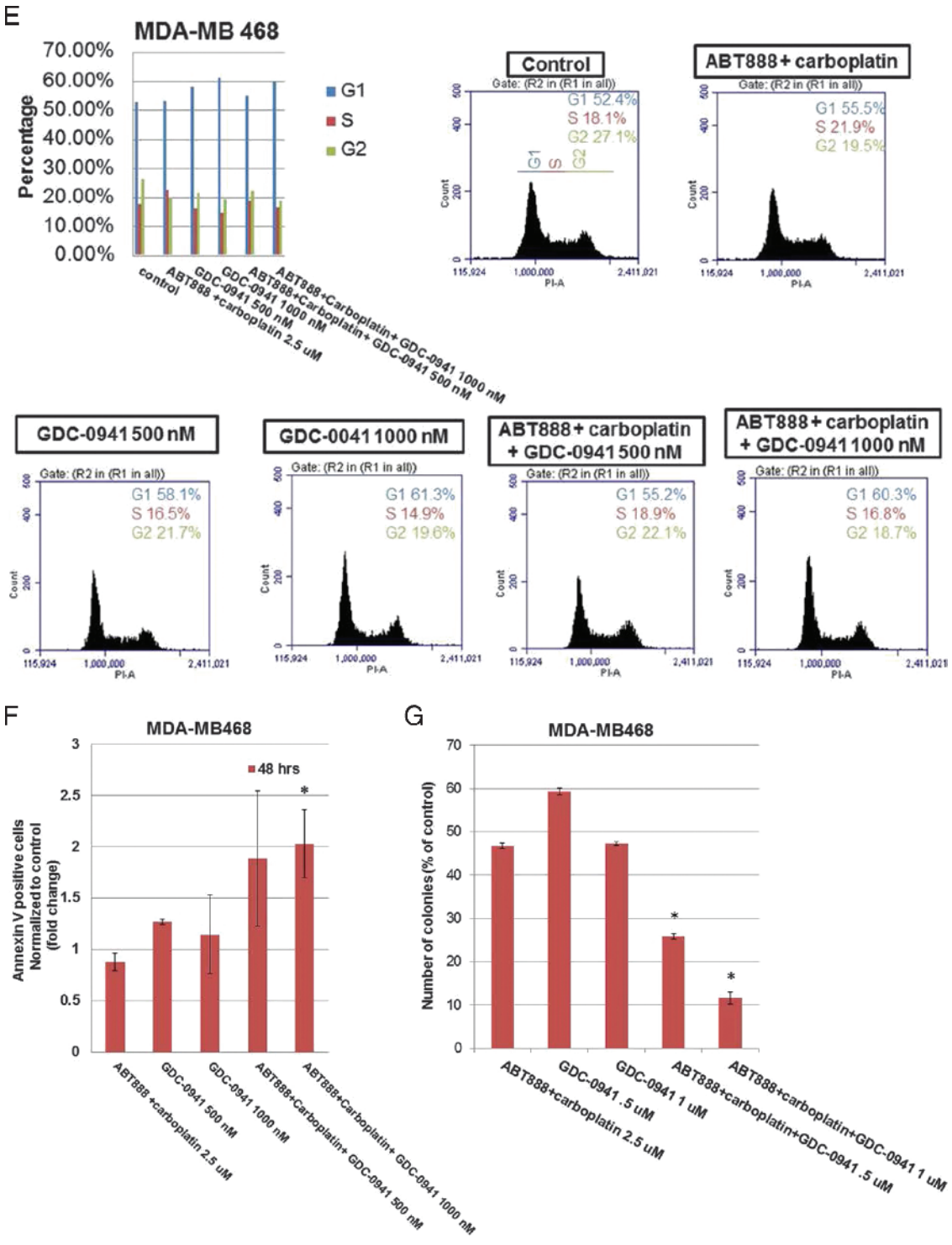

Figure 3. (*continued*).

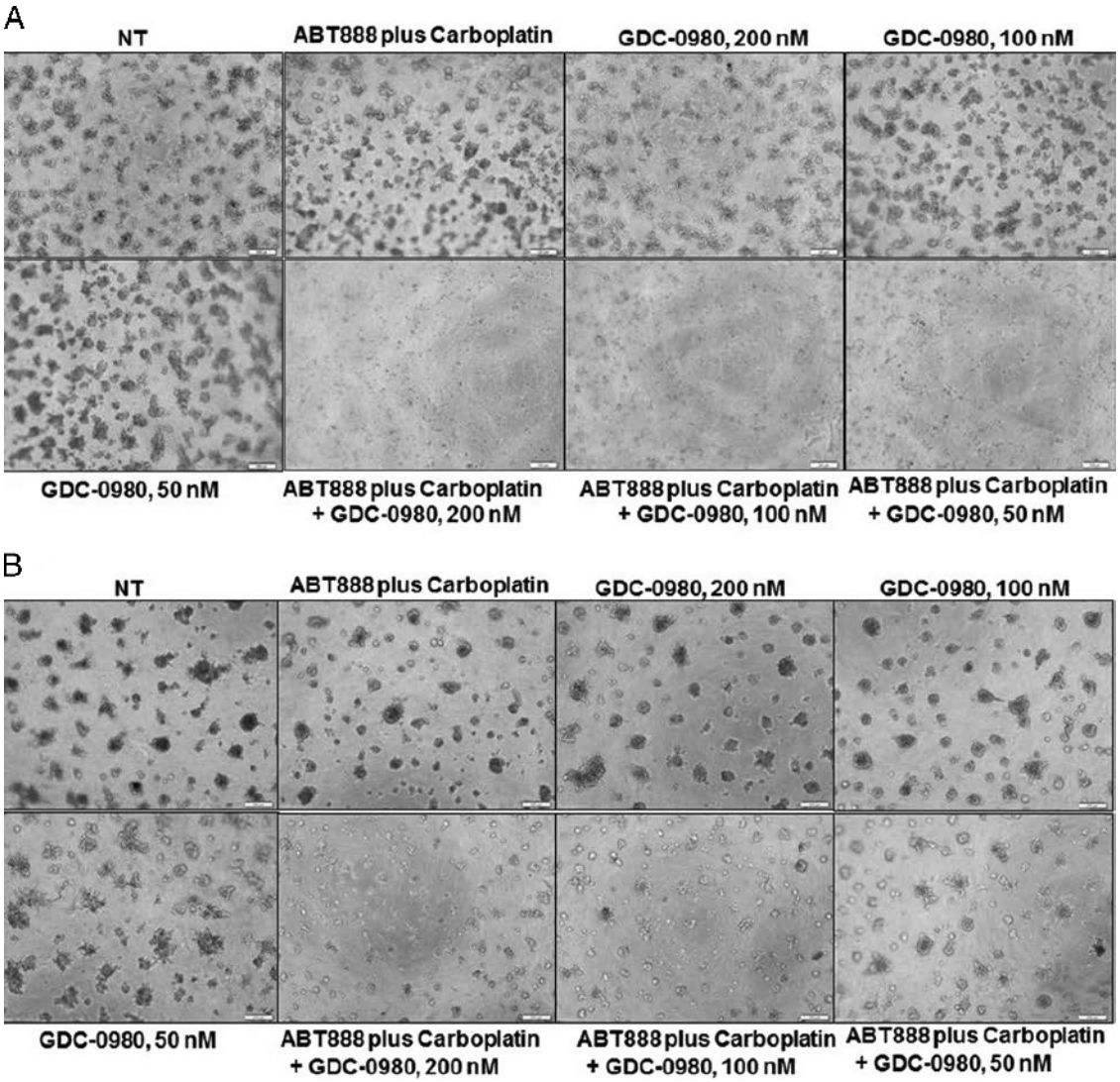

Figure 4. Effect of GDC-0980 alone and in combination with ABT888 plus carboplatin on clonogenic growth under anchorage-dependent and anchorage-independent conditions in BRCA-competent TNBC cells. MDA-MB468 (A) and MDA-MB231 cells (B) were plated under anchorage-dependent conditions (3D ON-TOP assay) for 7 days and pictures of live colonies were taken (Olympus DP32; original magnification, ×4). (C) Cells were plated in anchorage-independent conditions (soft agar assay) for 10 to 15 days with medium changes. Cell colonies were counted using an automatic gel counter. Data represent bar diagrams of the number of colonies (percentage of controls) in the respective groups of three independently performed experiments. D shows the schematic representation of the concept of combination of dual PI3K-mTOR inhibitor with PARPi plus carboplatin in TNBC. Tumor cells of TNBC have high mitotic index. The high mitotic index in these cells is maintained by 1) increased cell survival/proliferative signals, 2) decreased apoptosis signals, 3) decreased genotoxic exposure, 4) high-fidelity transmission of genetic information through error-free maintenance of replicating DNA, and 5) a conducive nutritional state, metabolic state, and protein/fatty acid synthesis. We provide a model to counter this oncogenic event by a combination of dual PI3K-mTOR inhibitor and PARPi plus carboplatin in TNBC cells. The model is derived from the concept that to ensure the high-fidelity transmission of genetic information, tumor cells have evolved mechanisms to respond to DNA damage by activating a complex DNA damage response pathway that includes cell cycle arrest, the transcriptional and post-transcriptional activation of a subset of genes including those associated with DNA repair. The simple corollary that emerged from the concept of "synthetic lethality" as proposed by Tutt et al., in the context of PARPi, is that tumor cells with high mitotic rates have a natural limit to withstand the extent of DNA damage and a limited capacity to respond to the DNA damage that needed to be corrected before cells enter into the mitosis. The model is based on the fact that an inability to respond properly to or repair DNA damage leads to triggering of programmed cell death and apoptosis. The model predicts that 1) the load of DNA damage will be increased by carboplatin treatment, 2) cells' capacity to repair the damaged DNA will be limited following PARP inhibition and PI3K inhibition, 3) dual PI3K-mTOR inhibitor will decrease survival and proliferative signals in cells and reduce cells' ability to respond to the posing nutritional/metabolic/protein synthesis load pertinent to the mitosis, and 4) inhibition of mTOR, a homeostatic ATP sensor of the cell integrating nutrient/energy signaling with that of growth factor signaling, will decrease proliferative signals in cells. The combination treatment with a dual PI3K-mTOR inhibitor and PARPi plus carboplatin in a tumor cell will incline the balance toward the proapoptosis state from the promitosis state.

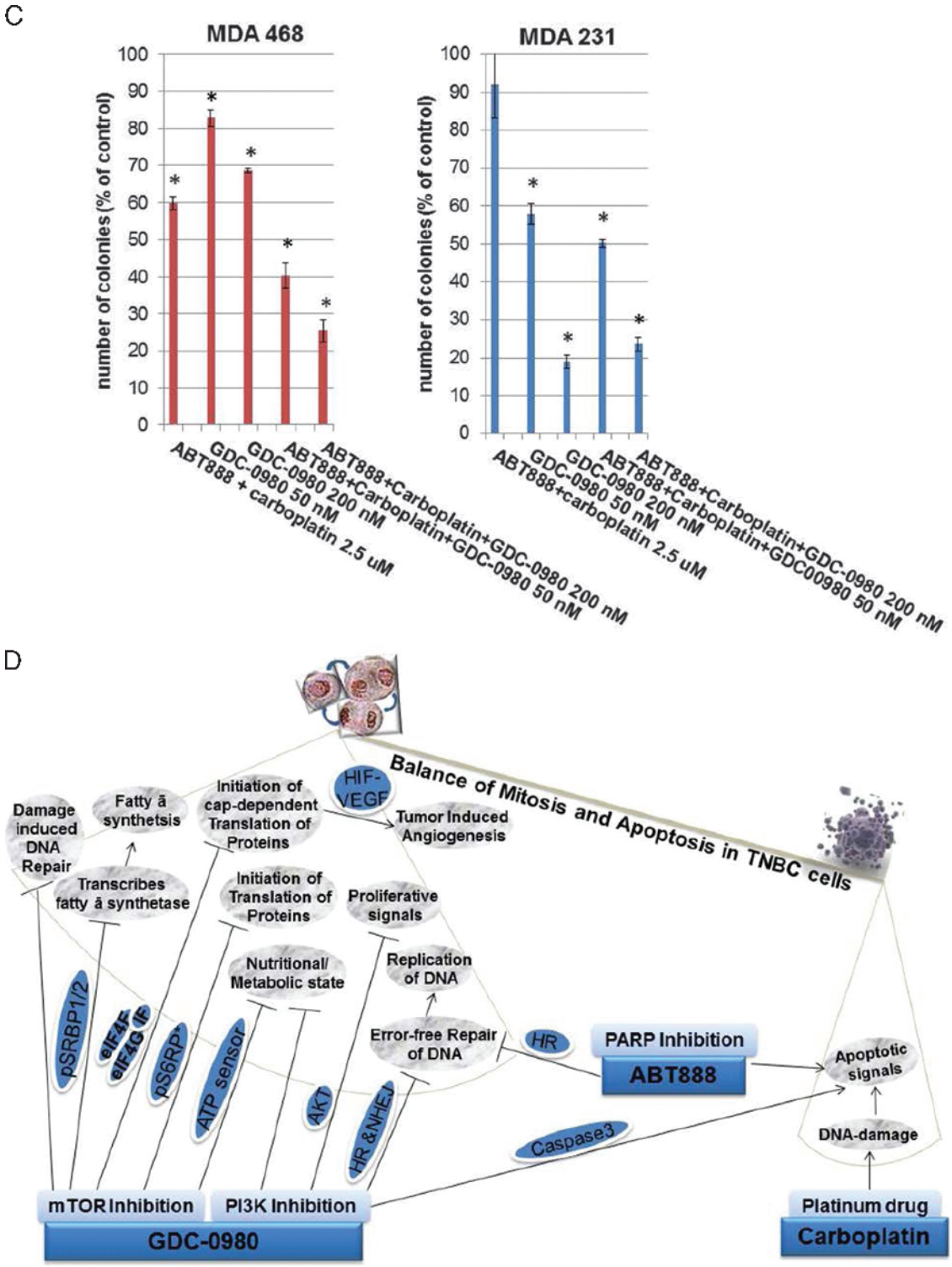

Figure 4. (*continued*).

apoptosis marker (cleaved caspase 3), and angiogenic markers (CD31 and pVEGFR) were determined by IHC from the formalin fixed paraffin embedded (FFPE) sections of the tumors obtained from the animals (each arm of the xenograft study). High expression of Ki67 has been associated with worse outcomes, and the measurement of Ki67 index pre-therapy and post-therapy provided an accurate surrogate for responsiveness of BC to the treatment [39]. PD studies showed a decrease in the Ki67, CD31, and pVEGFR expression with a concomitant increase in cleaved caspase 3 staining in tumors from mice treated with GDC-0980 in combination with ABT888 plus carboplatin compared to the control (Figures 5, *B–E*, and 6, *B–E*). The maximum antitumor effect of GDC-0980 was achieved in the MDA-MB468 xenograft model, which recapitulated with the tumor volumes (Figures 5*A* and 6*A*). Collectively, GDC-0980

in combination with ABT888 plus carboplatin showed an on-target activity in BRCA-proficient TNBC tumor models and more so in models wherein the PI3K-mTOR pathway is activated because of the loss of PTEN protein. These results, in agreement with the *in vitro* observation, showed that GDC-0980 in combination with ABT888 plus carboplatin was an efficacious antitumor drug combination in BRCA-competent TNBC model, especially with a PTEN-null background.

Antitumor Effect of the Combination of GDC-0980 with ABT888 plus Carboplatin Was Associated with the PD Knockdown of Phosphorylated S6RP$^{S235/236}$ and Phosphorylated 4EBP1$^{T37/46}$

Because our *in vitro* data showed that the combination treatment with ABT888, carboplatin, and GDC-0980 dose and time dependently blocked several key oncogenic molecules of the PI3K-mTOR

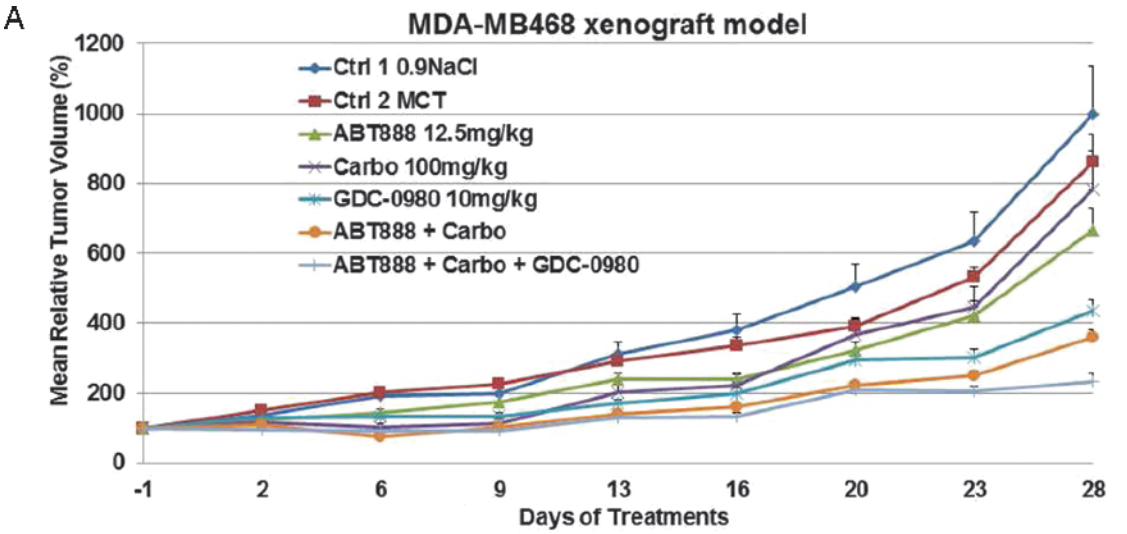

Arms of Treatments	MDA-MB468 xenograft model		
	Tumor volume (mm^3 ± SEM)	Significant (p value)	Body weight (gram ± SEM)
1. Control ,0.9% NaCl (pH 4.0), oral gavage, Bid, for 5 days	1346 ± 138		22.0 ± 0.09
2. Control , MCT, oral, every other day for 4 weeks (100 µl)	1114 ± 78.5		21.5 ± 0.11
3. ABT888 12.5 mg/kg in 0.9% NaCl (pH 4.0), oral gavage, Bid, for 5 days	911.5 ± 60.4	$p < 0.1754$	21.3 ± 0.18
4. Carboplatin 100 mg/kg, i.v. once	1059 ± 109	$p < 0.1915$	21.0 ± 0.23
5. GDC-0980 10 mg/kg in 100 µl, oral, every other day	584.3 ± 28.9	$p < 0.0610$	21.6 ± 0.21
6. ABT888 12.5 mg/kg + Carboplatin 100 mg/kg	500.8 ± 19.0	$p < 0.0334$	21.9 ± 0.11
7. GDC-0980 10 mg/kg + ABT888 12.5 mg/kg + Carboplatin 100 mg/kg	315.5 ± 22.9	$p < 0.0191$	21.8 ± 0.33

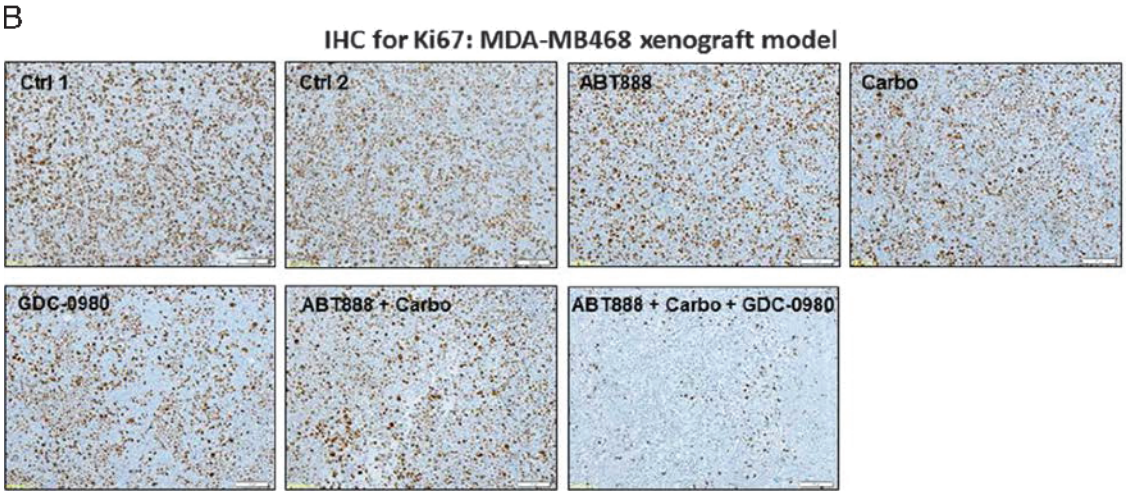

Figure 5. Efficacy of GDC-0980 alone and in combination with ABT888 plus carboplatin in a human tumor MDA-MB468 xenograft model. A pilot study was conducted to determine 1) the number of cells required to inject for the establishment of tumors and their maintenance in animals throughout the period of drug administration and 2) the maximum tolerable dose of drugs in animals with tumor burden. The number of cells injected was adjusted on the basis of the tolerable tumor burden in untreated animals (following IACUC guidelines). On the basis of the results of the pilot study, cells (MDA-MB468) were injected in matrigel subcutaneously into the flank of immunocompromised female nude (*nu/nu*) mice. Established xenograft tumors were treated with GDC-0980 (10 mg/kg, oral, every other day) alone and in combination with ABT888 (12.5 mg/kg in 0.9% NaCl [P^H4.0], oral gavage, twice a day, for 5 days) plus carboplatin (100 mg/kg, i.v. once) (A). The table (lower panel of A) shows the change in volumes of MDA-MB468 xenograft tumors and body weights of the mice in response to drug combinations. PD data for Ki67 (B), CD31 (C), pVEGFR (D), and cleaved caspase 3 (E) were presented.

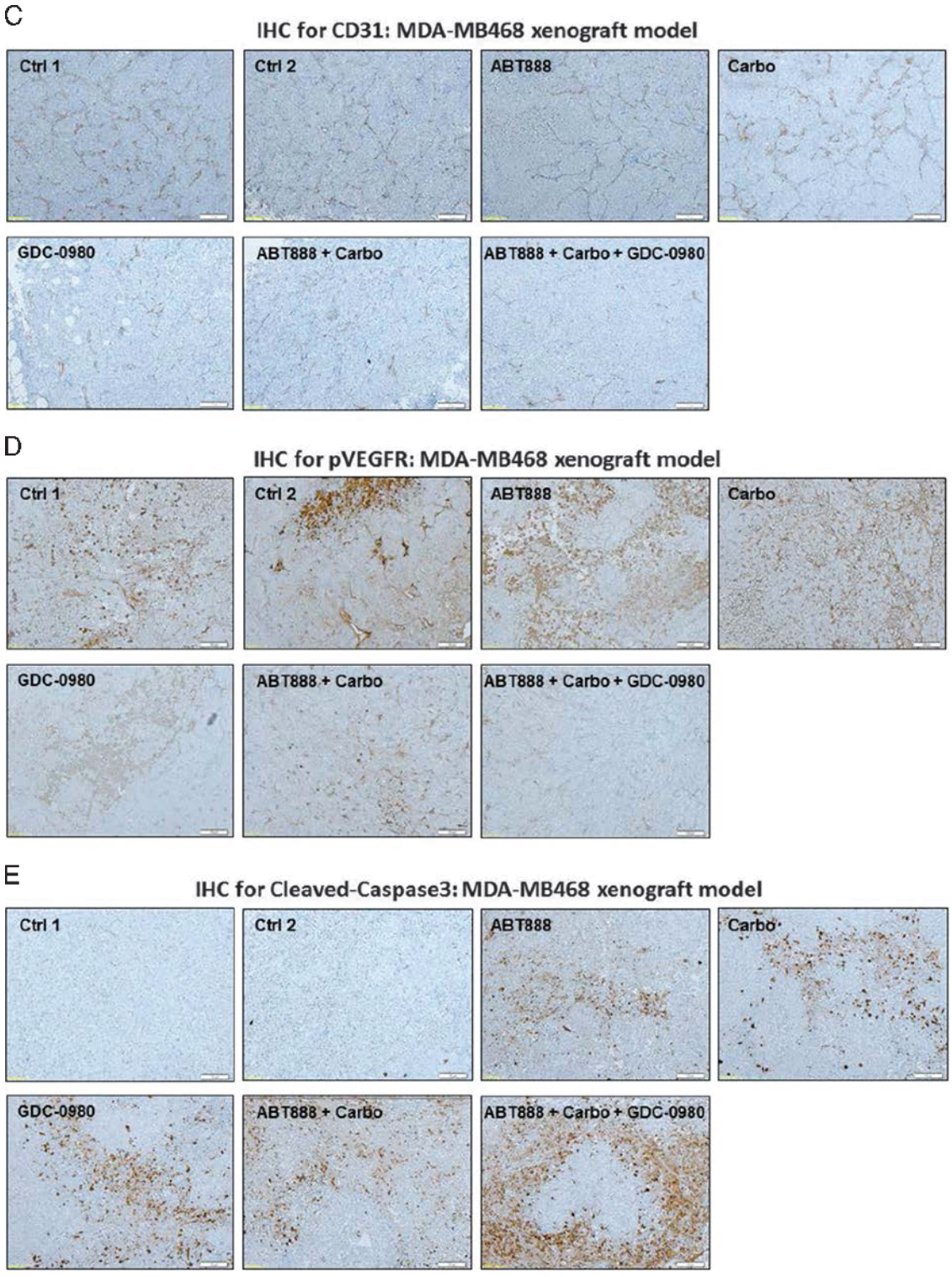

Figure 5. (*continued*).

pathway that were responsible for signaling the proliferation of tumor cells including phosphorylated S6RP$^{S235/236}$ and phosphorylated 4EBP1$^{T37/46}$, we also tested the levels of phosphorylated S6RP$^{S235/236}$ and phosphorylated 4EBP1$^{T37/46}$ in the FFPE sections from tumor samples obtained from xenograft studies (Figures 5*A* and 6*A*). Our PD data demonstrated that phosphorylated S6RP$^{S235/236}$ and phosphorylated 4EBP1$^{T37/46}$ were decreased following the treatment of the tumor-bearing mice with ABT888, carboplatin, and GDC-0980 in both xenograft models (Figure 7, *A*–*D*). Results showed that although no changes in the levels of phosphorylated S6RP$^{S235/236}$ and phosphorylated 4EBP1$^{T37/46}$ were observed after the treatment with ABT888 alone, the treatment of both carboplatin alone and GDC-0980 alone as well as their combinations clearly decreased the IHC levels of phosphorylated S6RP$^{S235/236}$ and phosphorylated 4EBP1$^{T37/46}$. As expected, the highest levels of inhibition were observed following the triple combination of ABT888, carboplatin, and GDC-0980.

Discussion

DDR machinery is fundamental to processes of tumorigenesis [40]. PARPi sensitivity and synthetic lethality have been reported to be circumstantial to the loss of BRCA-ness [41]. We tested our hypothesis that a node-specific inhibition of the PI3K pathway by GDC-0980 in the presence of carboplatin would result in 1) an enhanced impairment of DSB repair and 2) a subsequent sensitization to PARPi. This effect occurring simultaneously with the inhibition of classic PI3K-mTOR survival signal(s) would induce a robust antiproliferative/proapoptotic signal(s) in BRCA-competent TNBC cells. Thus, GDC-0980, in

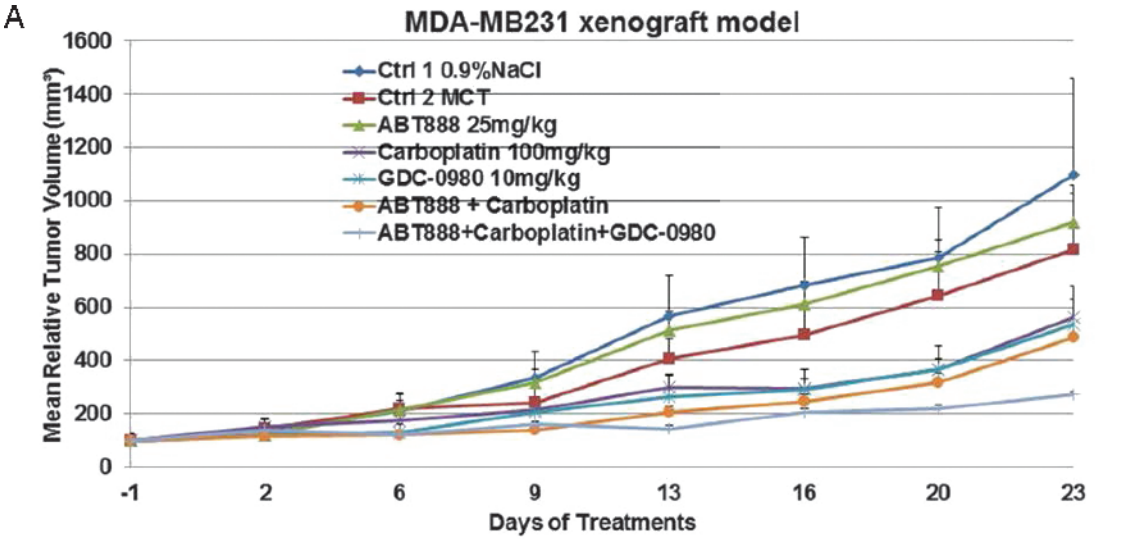

Arms of Treatments	MDA-MB231 xenograft model		
	Tumor volume (mm^3 ± SEM)	Significant (p value)	Body weight (gram ± SEM)
1. Control ,0.9% NaCl (pH 4.0), oral gavage, Bid, for 5 days	2175 ± 190.8		24.5 ± 0.59
2. Control , MCT, oral, daily for 4 weeks.(100 µl)	1837 ± 162.8		25 ± 0.18
3. ABT888 25 mg/kg in 0.9% NaCl (pH 4.0), oral gavage, Bid, for 5 days	1885 ± 98.4	$p < 0.4381$	24.3 ± 0.32
4. Carboplatin 100 mg/kg, i.v. once	1153 ± 39.3	$p < 0.0766$	25.4 ± 0.25
5. GDC-0980 10 mg/kg in 100 µl, oral, daily	1137 ± 88.9	$p < 0.0958$	23.8 ± 0.35
6. ABT888 25 mg/kg + Carboplatin 100 mg/kg	996.9 ± 32.7	$p < 0.0624$	23.7 ± 0.25
7. GDC-0980 10 mg/kg + ABT888 25 mg/kg + Carboplatin 100 mg/kg	193.7 ± 12.3	$p < 0.0022$	22.8 ± 0.09

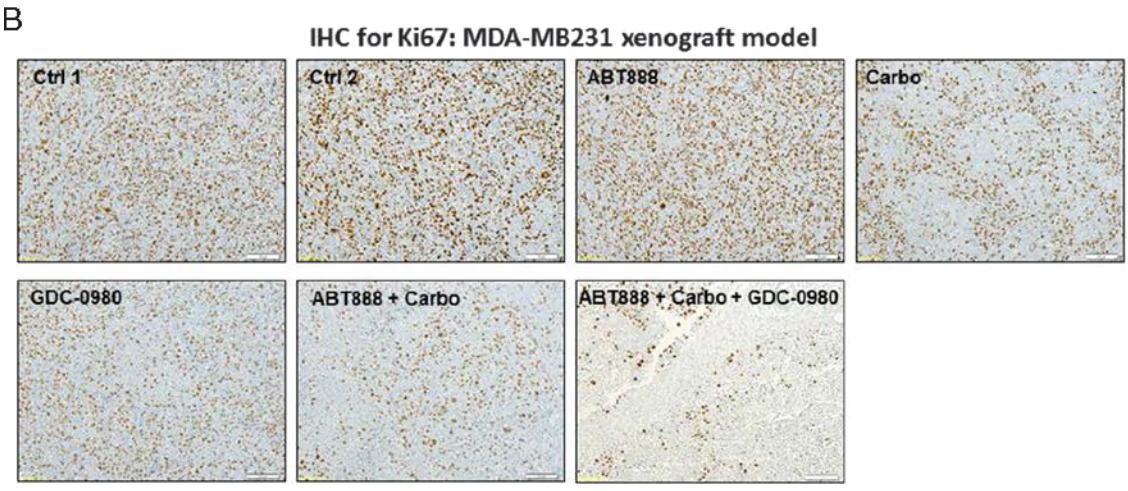

Figure 6. Efficacy of GDC-0980 alone and in combination with ABT888 plus carboplatin in a human tumor MDA-MB231 xenograft model. A pilot study was conducted to determine 1) the number of cells required to inject for the establishment of tumors and their maintenance in animals throughout the period of drug administration and 2) the maximum tolerable dose of drugs in animals with tumor burden. The number of cells injected was adjusted on the basis of the tolerable tumor burden in untreated animals (following IACUC guidelines). On the basis of the results of the pilot study, cells (MDA-MB231) were injected in matrigel subcutaneously into the flank of immunocompromised female nude (*nu/nu*) mice. Mice bearing breast cancer xenografts were treated with GDC-0980 (10 mg/kg, oral, daily) alone and in combination with ABT888 (25 mg/kg in 0.9% NaCl [P^H4.0], oral gavage, twice a day, for 5 days) plus carboplatin (100 mg/kg, i.v. once) (A). The table (lower panel of A) shows the change in volumes of MDA-MB231 xenograft tumors and body weights of the mice in response to drug combinations. PD data for Ki67 (B), CD31 (C), pVEGFR (D), and cleaved caspase 3 (E) were presented. A comparison between the efficacies of GDC-0980 and GDC-0941 in combination with ABT888 plus carboplatin tested in a human tumor MDA-MB231 xenograft model was presented (F). For the PD studies, tumors were analyzed for the markers shown at the end of the treatment period.

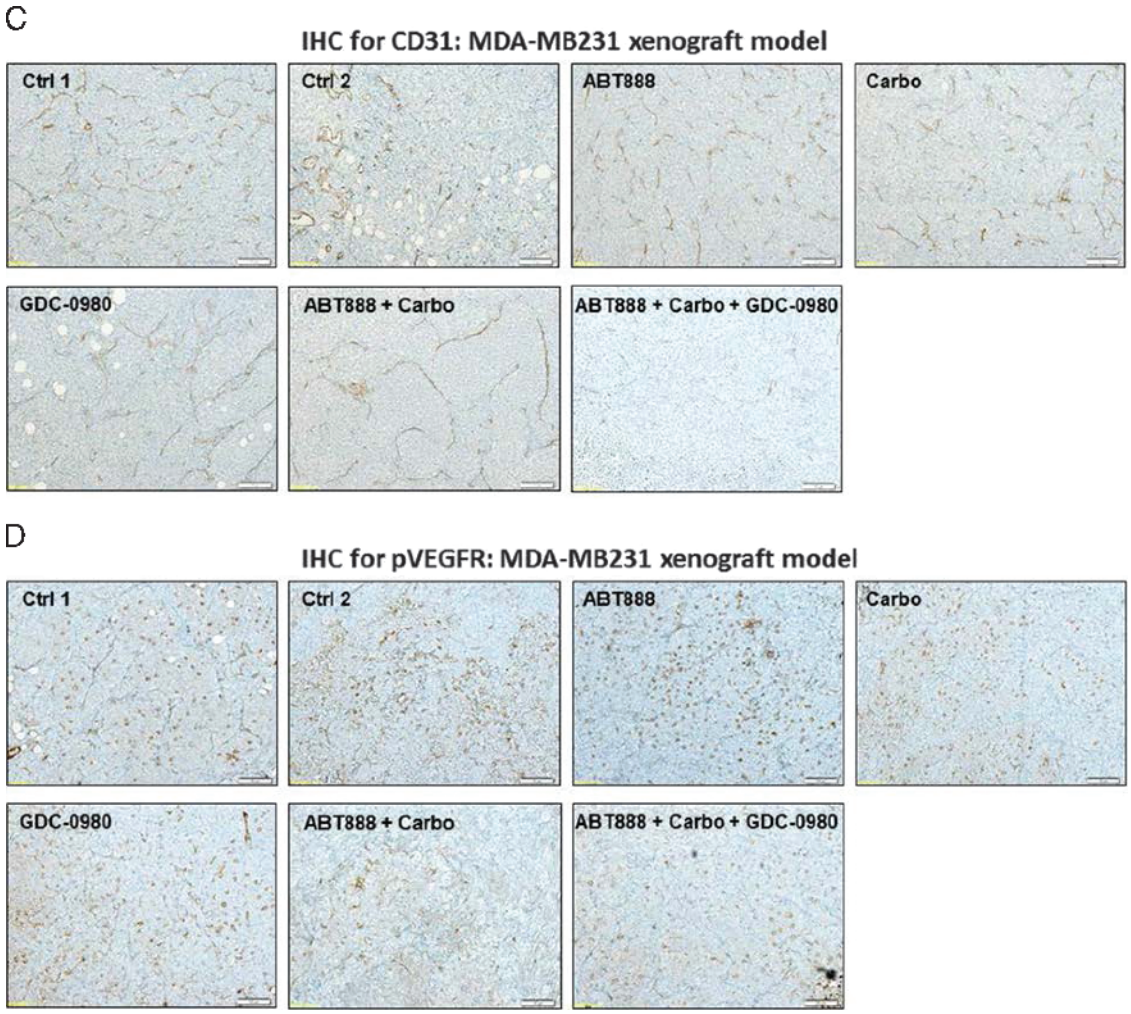

Figure 6. (*continued*).

combination with ABT888 plus carboplatin, profoundly attenuated the growth of TNBC tumors *in vivo*. Here, we report for the *first time* that a node-specific inhibition of the PI3K-mTOR pathway by GDC-0980 caused an impairment of DSB repair and resulted in a consequent sensitization to ABT888 plus carboplatin treatment in a BRCA-competent TNBC model (Figure 4*D*, schematics).

DNA damage (pγH2AX^{S139} foci, a marker of DSB) might cause an increased PAR polymer formation through PARP activation. Increased PAR levels along with increased ratios of PAR/PARP in both MDA-MB468 (Figure 1) and MDA-MB231 (Figures W2–W4) following the inhibition of PI3K and mTOR strongly indicated an altered state of DNA damage/DNA repair. Because PI3K is reported to control DSB repair and mTOR inhibition resulted in a significant suppression of both HR and NHEJ, the increased PAR level (indicating increased activation of PARP) and pγH2AX^{S139} levels following GDC-0980 in our result could be explained by a disconcerted DDR in the cell. The result that GDC-0980 alone induced PAR-rylation and enhanced the ratio of PAR/PARP in TNBC cells, and GDC-0980–induced PAR-rylation in BRCA-competent TNBC cells was blocked by ABT888 (Figure 1) together indicated that *the enhancement of DNA-damaging effects in the presence of GDC-0980 were not directly mediated through PARP inhibition*. In this context it is worth mentioning that IC_{50} of GDC-0980 for DNA-PKcs (DDR enzyme responsible for NHEJ) was previously reported in the nanomolar range similar to that for PI3K and mTOR kinase [42].

A dose-dependent increase in pγH2AX^{S139} only at 3 and 24 hours was observed in MDA-MB468, which was stabilized around 72 hours of treatment of GDC-0980. Although we observed maximum PAR formation and PAR/PARP ratio at 72 hours following GDC-0980 in MDA-MB468 cells, pγH2AX^{S139} levels were restored to near control at the same time (Figure 1). This indicated that the highest activation of PARP as a result of presumably more DNA damage (over 72 hours) did not lead to an increased/sustained DSB at 72 hours indicating, at this longer time point, that a cellular equilibrium of DNA damage/DDR was achieved in this cell. It is possible that the DSBs were repaired and restored by the BRCA-proficient RAD51 system of the cell. Our argument is further supported by the fact that the same doses of GDC-0980 when combined with ABT888 and carboplatin induced a robust increase in pγH2AX^{S139} at 72 hours along with the concomitant increase in 1) apoptosis markers (cleaved caspases 3 and 9, cleaved PARP, and BIM), 2) annexin V positivity, (3) percentage of dead cells, and (4) IF of cleaved caspase 3.

We observed a characteristic difference between the responses of MDA-MB231 and MDA-MB468 cells to the drugs in terms of PAR and pγH2AX^{S139} levels and their ratios. PTEN-null MDA-MB468 cells were observed to be more sensitive and dose responsive not only

to the GDC-0980 treatment alone but also to the combination(s) compared to RAS/RAF-mutated MDA-MB231 cells. There is an accumulating body of evidence implicating the MAPK signaling pathway in DNA repair and cell survival [43]. Weidhaas et al. [44] have reported that the RAS/MAPK pathway signaling was genetically linear with the DNA damage response pathway and acted downstream of the DNA damage checkpoint implicating involvement of this pathway in DDR following cytotoxic drugs. Oncogenic HRAS has been reported to enhance DNA repair [45]. DDR genes were upregulated after epidermal growth factor receptor (EGFR)/RAS/MAPK signaling [46,47]. There is measurable decrease in DNA repair with EGFR pathway inhibition, and gefitinib treatment was accompanied by inhibition of DDR and cell growth in oral cancer [48]. In fact, tumors mediated by activating mutations or overexpression of components of the EGFR signaling pathway were all found to be resistant to cytotoxic therapy [49,50]. Our findings indicate that enhanced repair of damage/resistance to response to DNA-damaging drugs and PARPi in the tumor cell may be associated with an upregulated RAS/MAPK pathway.

However, the absence of PTEN protein might also have contributed to the increased sensitivity and dose responsiveness in our study not only to GDC-0980 treatment alone but also to the combinations owing to PTEN's transcriptional effect on the BRCA-RAD51 system and its effect on genetic stability [51]. Shen et al. suggested a direct impact of PTEN on transcriptional regulation of RAD51 [52], and Baker reported increased nuclear foci of pγH2AX^{S139} following

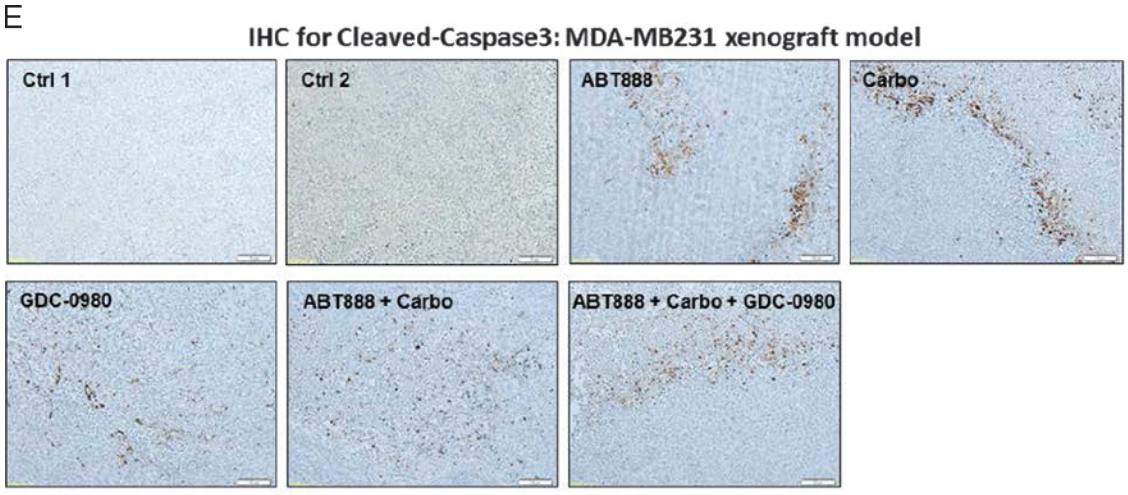

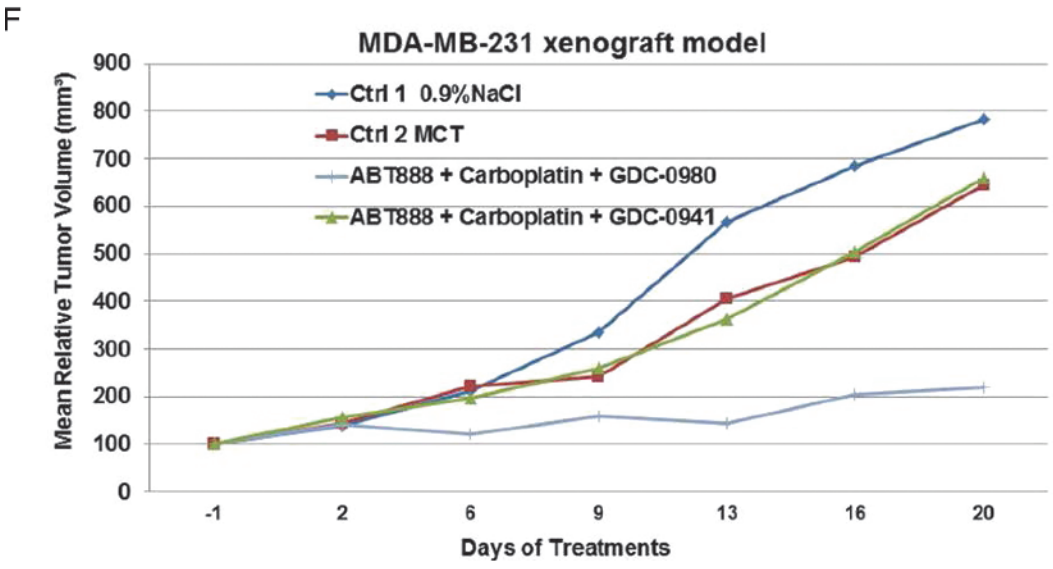

Arms of treatments	MDA-MB-231 xenograft model		
	Tumor volume (mm³ ± SEM)	Significant (*p* value)	Body weight (gram ± SEM)
1. Control ,0.9% NaCl (PH4.0), oral gavage, Bid, for 5 days	1553 ± 176.7		24.5 ± 0.59
2. Control , MCT, oral, daily for 4 weeks.(100µl)	1446 ± 97.83		25 ± 0.18
3. GDC-0980 10 mg/kg + ABT888 25mg/kg + Carboplatin 100mg/kg.	157.2 ± 15.48	$p < 0.0022$	22.8 ± 0.09
4. GDC-0941 10 mg/kg + ABT888 25mg/kg + Carboplatin 100mg/kg.	1195 ± 23.60	$p < 0.4738$	21.8 ± 0.95

Figure 6. (*continued*).

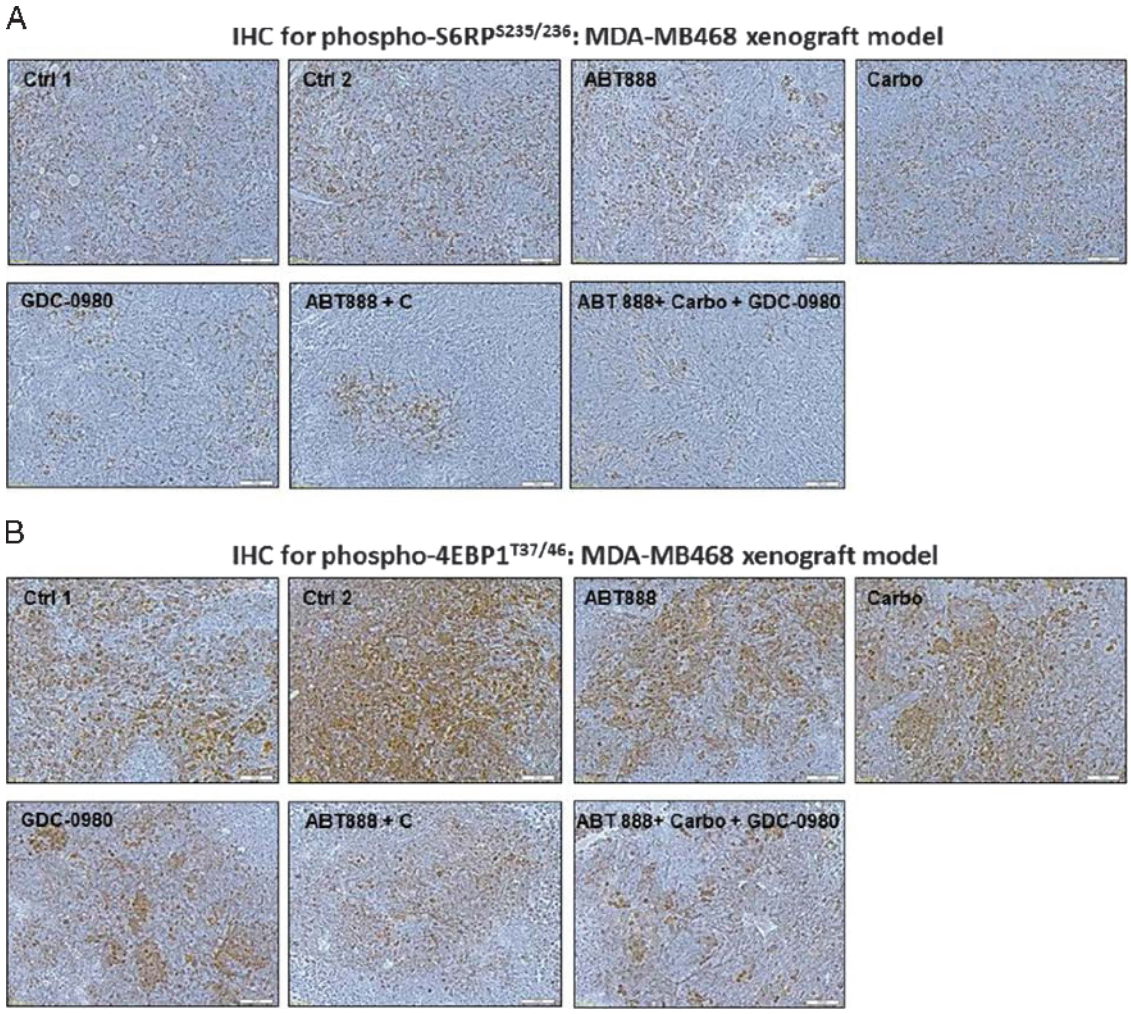

Figure 7. The PD knockdown of phosphorylated S6RP$^{S235/236}$ and phosphorylated 4EBP1$^{T37/46}$ *in vivo* following the treatment of GDC-0980 alone and in combination with ABT888 plus carboplatin. Mice bearing breast cancer xenografts of TNBC cells (MDA-MB231 and MDA-MB468) were treated with GDC-0980 (10 mg/kg, oral, daily) alone and in combination with ABT888 (25 mg/kg in 0.9% NaCl [P^{H}4.0], oral gavage, twice a day, for 5 days) plus carboplatin (100 mg/kg, i.v. once). PD data for phosphorylated S6RP$^{S235/236}$ (A and C) and phosphorylated 4EBP1$^{T37/46}$ (B and D) for MDA-MB468 (A and B) and MDA-MB231(C and D) were presented. For the PD studies, tumors were analyzed for the markers shown at the end of the treatment period.

PTEN RNAi [53]. A genetic inactivation of PTEN suppressed DNA repair to induce a synergistic effect of olaparib in combination with cisplatin [54]. Taken together, it is possible that the PTEN nullness in our cells had a permissive role in mediating the effect of the combination of GDC-0980 and ABT888 plus carboplatin. In the context of TNBC, this has particular therapeutic/translational relevance due to two reasons. First, the team of Kornelia Polyak [4] has recently demonstrated the importance of PTEN loss in the relative temporal order of somatic events associated with the basal-like subtype to show that PTEN loss is the most common first event. Second, loss of PTEN protein is observed in a significant percentage of the TNBC patient population [6,51,55].

Inhibition of apoptosis through interaction with DDR enzyme–associated signaling complex has been reported in human cancer cells [56]. The differences in response to the drug combination in survival/proliferative signals between the two cell lines can be explain by the RAS/RAF status of MDA-MB231 as previously reported by Wallin et al. [57]. There is a regulatory mechanism for balancing p53 and RAS/MAPK signaling [58]. Since inhibition of AKT leads to transcriptional activation of receptor tyrosine kinases (RTKs) through FOXO [59], we tested the phosphorylation status of EGFR/total EGFR following GDC-0980. However, no change was observed in pEGFR in our model system. The limited long-term (72 hours) effect of GDC-0980 on direct downstream of mTOR, p4EBP1$^{T37/46}$, and pP70S6K may be explained by a higher IC_{50} of GDC-0980 for mTORC kinase than PI3K as reported earlier [42]. In a sharp contrast to MDA-MB468 cells, there was an absence of induction of cleaved PARP and also of other effectors of apoptosis including cleaved caspase 9 and BIM at any time following treatment in MDA-MB231 cells as reported in an earlier observation [57]. Whether the observed differences between cell lines were attributed to their basal-like (MDA-MB468) or mesenchymal-like (MDA-MB231) behavior as recently reported by Yi et al. [60] or were attributed to the KRAS/BRAF pathway–mediated resistance for GDC-0980 [57] remains to be determined.

Consistent with our *in vitro* results, GDC-0980 in combination with ABT888 plus carboplatin was found to be more efficacious in the MDA-MB468 xenograft model when compared to MDA-MB231. We observed a higher half maximal effective concentration

(EC_{50}; 5 μM) value for GDC-0980 in this cell line in our study (Figure W1) consistent with an earlier report [57]. The limited effect to MDA-MB231 cells of the combination may be due in part by its limited effect on cell cycle progression, ineffectiveness to induce downstream apoptosis markers, lack of apoptosis, and high live/dead cell ratios *in vitro*. In addition, the combination also had limited effect on PAR formation and levels of $p\gamma H2AX^{S139}$ in MDA-MB231. One of the reasons that GDC-0980 alone had a limited effect on MDA-MB231 was that it is a dual PI3K-mTOR inhibitor and cells with RAS/RAF mutation background are specifically insensitive to PI3K inhibitors. In line with this rationale, we observed that pan-PI3K inhibitor GDC-0941 failed to show any efficacy in an MDA-MB231 xenograft model (Figure 6*F*). This was consistent with a previous report that in KRAS-mutant cells with an activated RAS/MAPK pathway, survival is primarily mediated through the MAPK pathway and potent inhibition of MAPK even with modest inhibition of AKT could drive an increase in apoptosis [61]. Similarly, we also failed to identify an up-regulation of any apoptotic marker(s) in our *in vitro* experiments. Our PD data demonstrated that IHC expression of cleaved caspase 3 in the tumors from the MDA-MB468 xenograft model is higher compared to the matched controls in the tumors from the MDA-MB231 model (Figures 5 and 6). Vijapurkar et al. demonstrated that mTOR kinase inhibition had potent cytostatic effect but did not induce apoptosis as a result of negative feedback inhibition and/or maintenance of survival signaling. A significant cytotoxicity was induced by a co-targeting mTOR kinase with the specific survival pathways in diagnostically defined subpopulations, i.e., the PI3K pathway in PI3K-mutant cells or the MAPK pathway in KRAS-mutant cells [61]. Our PD data showed that highest levels of the inhibition of phosphorylated $S6RP^{S235/236}$ and phosphorylated $4EBP1^{T37/46}$ occurred in the tumors of the mice treated with the triple combination of ABT888, carboplatin, and GDC-0980 (Figure 7). This result demonstrates the capacity of the combination of ABT888, carboplatin, and GDC-0980 to affect a sustained knockdown of phosphorylated $S6RP^{S235/236}$ and phosphorylated $4EBP1^{T37/46}$ *in vivo* and indicates that the inhibition of the growth of the tumor is mediated through the inhibition of oncogenic signals like phosphorylated $S6RP^{S235/236}$ and phosphorylated $4EBP1^{T37/46}$.

In summary, we demonstrate that inhibition of DDR is another mode of action of GDC-0980, and when combined with PARPi plus carboplatin, GDC-0980 induces an effective antitumor effect in BRCA-competent TNBC cells. Our combination exhibited the potential to kill BRCA-competent TNBC cells because carboplatin-induced DNA damage was amplified by GDC-0980 and PARPi to make a large flux of DSB that overwhelm the normal DDR capacity of these tumor cells to induce apoptosis. Considering the importance of PARP as a

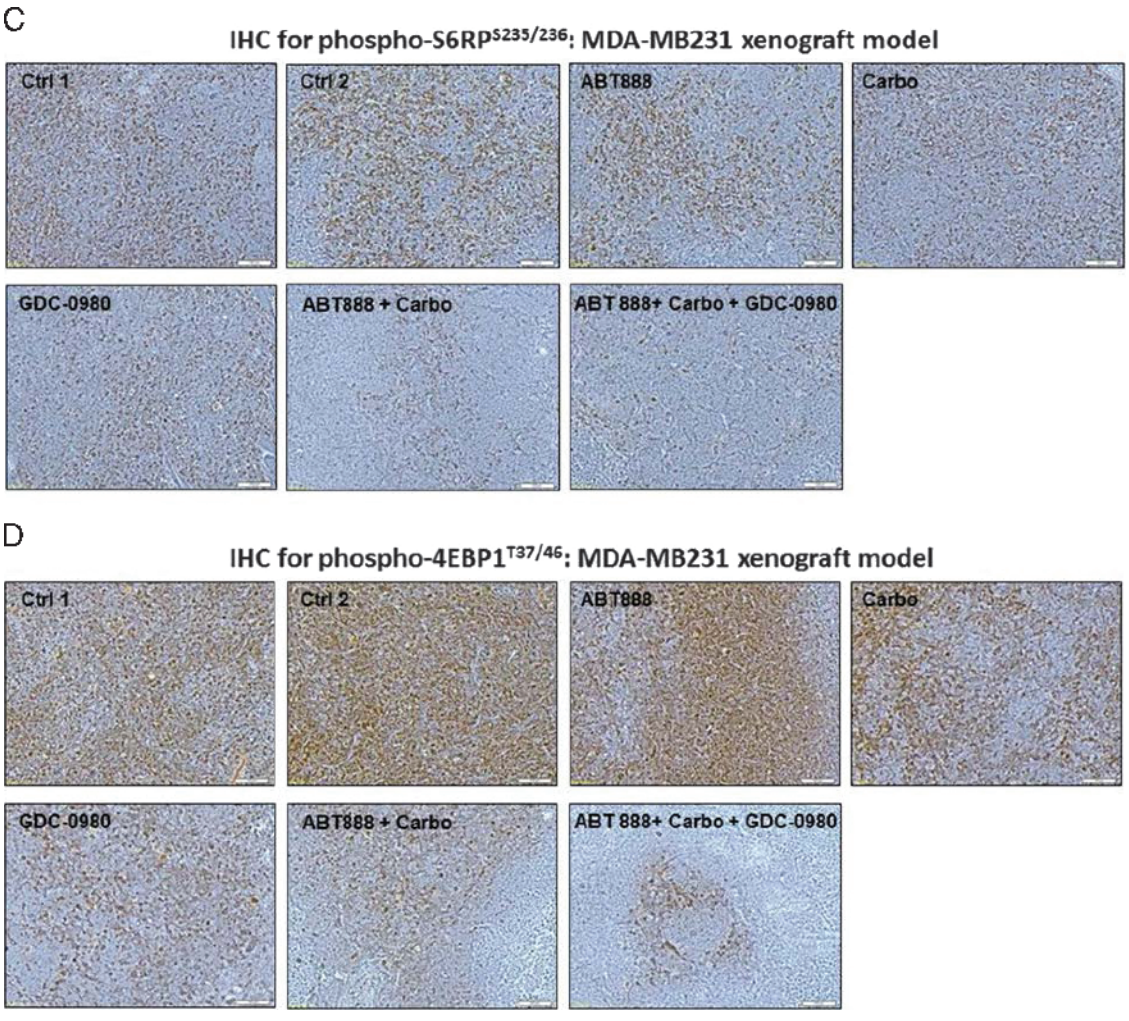

Figure 7. (*continued*).

target in TNBC, and the existence of a large percentage of BRCA-competent TN and/or basal-type BC patients, this combination has a promise toward the treatment of BRCA-competent TNBC and thus merits further investigation.

Acknowledgments

The authors thank Brian R. Smith and Casey Williams for critically reviewing the manuscript. The authors acknowledge the Department of Internal Medicine, USD (Vermilion, SD). The ABT888 for the *in vitro* study was received from NCI. The authors acknowledge the help of Kelly Graber (Confocal Core facilities of Sanford Research). The authors acknowledge the Flow Cytometry Core. The authors also thank Claire Evans (HT; the Molecular Pathology Core, supported by a grant from the NIH Center of Biomedical Research Excellence; grant 1P20RR024219-01A2). The authors also acknowledge Avera Cancer Institute for providing the financial support for the publication of the manuscript.

References

[1] Grigoriadis A, Mackay A, Noel E, Wu PJ, Natrajan R, Frankum J, Reis-Filho JS, and Tutt A (2012). Molecular characterisation of cell line models for triple-negative breast cancers. *BMC Genomics* **13**, 619.

[2] Boyle P (2012). Triple-negative breast cancer: epidemiological considerations and recommendations. *Ann Oncol* **23**(suppl 6), vi7–vi12.

[3] de Ruijter TC, Veeck J, de Hoon JP, van Engeland M, and Tjan-Heijnen VC (2011). Characteristics of triple-negative breast cancer. *J Cancer Res Clin Oncol* **137**, 183–192.

[4] Martins FC, De S, Almendro V, Gönen M, Park SY, Blum JL, Herlihy W, Ethington G, Schnitt SJ, Tung N, et al. (2012). Evolutionary pathways in BRCA1-associated breast tumors. *Cancer Discov* **2**, 503–511.

[5] Dey N, Smith BR, and Leyland-Jones B (2012). Targeting basal-like breast cancers. *Curr Drug Targets* **13**, 1510–1524.

[6] Jones N, Bonnet F, Sfar S, Lafitte M, Lafon D, Sierankowski G, Brouste V, Banneau G, Tunon de Lara C, Debled M, et al. (2013). Comprehensive analysis of PTEN status in breast carcinomas. *Int J Cancer* **133**, 323–334.

[7] Mao Z, Jiang Y, Liu X, Seluanov A, and Gorbunova V (2009). DNA repair by homologous recombination, but not by nonhomologous end joining, is elevated in breast cancer cells. *Neoplasia* **11**, 683–691.

[8] Pal SK, Childs BH, and Pegram M (2011). Triple negative breast cancer: unmet medical needs. *Breast Cancer Res Treat* **125**, 627–636.

[9] Tutt A, Robson M, Garber JE, Domchek SM, Audeh MW, Weitzel JN, Friedlander M, Arun B, Loman N, Schmutzler RK, et al. (2010). Oral poly (ADP-ribose) polymerase inhibitor olaparib in patients with BRCA1 or BRCA2 mutations and advanced breast cancer: a proof-of-concept trial. *Lancet* **376**, 235–244.

[10] Gartner EM, Burger AM, and Lorusso PM (2010). Poly(ADP-ribose) polymerase inhibitors: a novel drug class with a promising future. *Cancer J* **16**, 83–90.

[11] Tutt A, Robson M, Garber JE, Domchek S, Audeh MW, Weitzel JN, Friedlander M, and Carmichael J (2009). Phase II trial of the oral PARP inhibitor olaparib in BRCA-deficient advanced breast cancer. *J Clin Oncol (Meet Abstr)* **27**, CRA501.

[12] Farmer H, McCabe N, Lord CJ, Tutt AN, Johnson DA, Richardson TB, Santarosa M, Dillon KJ, Hickson I, Knights C, et al. (2005). Targeting the DNA repair defect in BRCA mutant cells as a therapeutic strategy. *Nature* **434**, 917–921.

[13] Fong PC, Boss DS, Yap TA, Tutt A, Wu P, Mergui-Roelvink M, Mortimer P, Swaisland H, Lau A, O'Connor MJ, et al. (2009). Inhibition of poly(ADP-ribose) polymerase in tumors from BRCA mutation carriers. *N Engl J Med* **361**, 123–134.

[14] Daemen A, Wolf DM, Korkola JE, Griffith OL, Frankum JR, Brough R, Jakkula LR, Wang NJ, Natrajan R, Reis-Filho JS, et al. (2012). Cross-platform pathway-based analysis identifies markers of response to the PARP inhibitor olaparib. *Breast Cancer Res Treat* **135**, 505–517.

[15] Kumar A, Fernandez-Capetillo O, and Carrera AC (2010). Nuclear phosphoinositide 3-kinase β controls double-strand break DNA repair. *Proc Natl Acad Sci USA* **107**, 7491–7496.

[16] Juvekar A, Burga LN, Hu H, Lunsford EP, Ibrahim YH, Balmana J, Rajendran A, Papa A, Spencer K, Lyssiotis CA, et al. (2012). Combining a PI3K inhibitor with a PARP inhibitor provides an effective therapy for BRCA1-related breast cancer. *Cancer Discov* **2**, 1048–1063.

[17] Ibrahim YH, García-García C, Serra V, He L, Torres-Lockhart K, Prat A, Anton P, Cozar P, Guzmán M, Grueso J, et al. (2012). PI3K inhibition impairs BRCA1/2 expression and sensitizes BRCA-proficient triple-negative breast cancer to PARP inhibition. *Cancer Discov* **2**, 1036–1047.

[18] Keith CT and Schreiber SL (1995). PIK-related kinases: DNA repair, recombination, and cell cycle checkpoints. *Science* **270**, 50–51.

[19] Beuvink I, Boulay A, Fumagalli S, Zilbermann F, Ruetz S, O'Reilly T, Natt F, Hall J, Lane HA, and Thomas G (2005). The mTOR inhibitor RAD001 sensitizes tumor cells to DNA-damaged induced apoptosis through inhibition of p21 translation. *Cell* **120**, 747–759.

[20] Dennis PB, Jaeschke A, Saitoh M, Fowler B, Kozma SC, and Thomas G (2001). Mammalian TOR: a homeostatic ATP sensor. *Science* **294**, 1102–1105.

[21] Hay N and Sonenberg N (2004). Upstream and downstream of mTOR. *Genes Dev* **18**, 1926–1945.

[22] De P, Miskimins K, Dey N, and Leyland-Jones B (2013). Promise of rapalogues versus mTOR kinase inhibitors in subset specific breast cancer: old targets new hope. *Cancer Treat Rev* **39**, 403–412.

[23] Mukherjee B, Tomimatsu N, Amancherla K, Camacho CV, Pichamoorthy N, and Burma S (2012). The dual PI3K/mTOR inhibitor NVP-BEZ235 is a potent inhibitor of ATM- and DNA-PKCs-mediated DNA damage responses. *Neoplasia* **14**, 34–43.

[24] Cardnell RJ, Feng Y, Diao L, Fan YH, Masrorpour F, Wang J, Shen Y, Mills GB, Minna JD, Heymach JV, et al. (2013). Proteomic markers of DNA repair and PI3K pathway activation predict response to the PARP inhibitor BMN 673 in small cell lung cancer. *Clin Cancer Res* **19**, 6322–6328.

[25] Herold CI and Anders CK (2013). New targets for triple-negative breast cancer. *Oncology* **27**, 846–854.

[26] Dey N, Barwick B, Moreno C, Ordanic-Kodani M, Chen Z, De P, Tang W, Catzavelos C, Kerstann K, Sledge GW, et al. (2013). Wnt signaling in triple negative breast cancer is associated with poor prognosis and metastasis. *BMC Cancer* **27**. DOI: 10.1186/1471-2407-13-537, E-pub ahead of print.

[27] Dey N, Young B, Abramovitz M, Bouzyk M, Barwick B, De P, and Leyland-Jones B (2013). Differential activation of Wnt-β-catenin pathway in triple negative breast cancer increases MMP7 in a PTEN dependent manner. *PLoS One* **8**, e77425.

[28] Dey N, De PK, Wang M, Zhang H, Dobrota EA, Robertson KA, and Durden DL (2007). CSK controls retinoic acid receptor (RAR) signaling: a RAR-c-SRC signaling axis is required for neuritogenic differentiation. *Mol Cell Biol* **27**, 4179–4197.

[29] Dey N, Howell BW, De PK, and Durden DL (2005). CSK negatively regulates nerve growth factor induced neural differentiation and augments AKT kinase activity. *Exp Cell Res* **307**, 1–14.

[30] Lee GY, Kenny PA, Lee EH, and Bissell MJ (2007). Three-dimensional culture models of normal and malignant breast epithelial cells. *Nat Methods* **4**, 359–365.

[31] Sun Y, Dey N, Brammer M, De P, and Leyland-Jones B (2013). Bevacizumab confers additional advantage to the combination of trastuzumab plus pertuzumab in trastuzumab-refractory breast cancer model. *Cancer Chemother Pharmacol* **72**, 733–745.

[32] Chen H, Ma Z, Vanderwaal RP, Feng Z, Gonzalez-Suarez I, Wang S, Zhang J, Roti Roti JL, Gonzalo S, and Zhang J (2011). The mTOR inhibitor rapamycin suppresses DNA double-strand break repair. *Radiat Res* **175**, 214–224.

[33] Ma W, Halweg CJ, Menendez D, and Resnick MA (2012). Differential effects of poly(ADP-ribose) polymerase inhibition on DNA break repair in human cells are revealed with Epstein-Barr virus. *Proc Natl Acad Sci USA* **109**, 6590–6595.

[34] Burma S, Chen BP, Murphy M, Kurimasa A, and Chen DJ (2001). ATM phosphorylates histone H2AX in response to DNA double-strand breaks. *J Biol Chem* **276**, 42462–42467.

[35] Hans MA, Müller M, Meyer-Ficca M, Bürkle A, and Küpper JH (1999). Overexpression of dominant negative PARP interferes with tumor formation of HeLa cells in nude mice: evidence for increased tumor cell apoptosis *in vivo*. *Oncogene* **18**, 7010–7015.

[36] Graeser M, McCarthy A, Lord CJ, Savage K, Hills M, Salter J, Orr N, Parton M, Smith IE, Reis-Filho JS, et al. (2010). A marker of homologous recombination predicts pathologic complete response to neoadjuvant chemotherapy in primary breast cancer. *Clin Cancer Res* **16**, 6159–6168.

[37] Yang SX, Kummar S, Steinberg SM, Murgo AJ, Gutierrez M, Rubinstein L, Nguyen D, Kaur G, Chen AP, Giranda VL, et al. (2009). Immunohistochemical detection of poly(ADP-ribose) polymerase inhibition by ABT-888 in patients with refractory solid tumors and lymphomas. *Cancer Biol Ther* **8**, 2004–2009.

[38] Bryant HE and Helleday T (2006). Inhibition of poly (ADP-ribose) polymerase activates ATM which is required for subsequent homologous recombination repair. *Nucleic Acids Res* **34**, 1685–1691.

[39] Kamel D, Brady B, Tabchy A, Mills GB, and Hennessy B (2012). Proteomic classification of breast cancer. *Curr Drug Targets* **13**, 1495–1509.

[40] Bartkova J, Horejsí Z, Koed K, Krämer A, Tort F, Zieger K, Guldberg P, Sehested M, Nesland JM, Lukas C, et al. (2005). DNA damage response as a candidate anti-cancer barrier in early human tumorigenesis. *Nature* **434**, 864–870.

[41] Montoni A, Robu M, Pouliot E, and Shah GM (2013). Resistance to PARP-inhibitors in cancer therapy. *Front Pharmacol* **4**, 18.

[42] Sutherlin DP, Bao L, Berry M, Castanedo G, Chuckowree I, Dotson J, Folks A, Friedman L, Goldsmith R, Gunzner J, et al. (2011). Discovery of a potent, selective, and orally available class I phosphatidylinositol 3-kinase (PI3K)/mammalian target of rapamycin (mTOR) kinase inhibitor (GDC-0980) for the treatment of cancer. *J Med Chem* **54**, 7579–7587.

[43] Upadhyay D, Bundesmann M, Panduri V, Correa-Meyer E, and Kamp DW (2004). Fibroblast growth factor-10 attenuates H_2O_2-induced alveolar epithelial cell DNA damage: role of MAPK activation and DNA repair. *Am J Respir Cell Mol Biol* **31**, 107–113.

[44] Weidhaas JB, Eisenmann DM, Holub JM, and Nallur SV (2006). A conserved RAS/mitogen-activated protein kinase pathway regulates DNA damage–induced cell death postirradiation in Radelegans. *Cancer Res* **66**, 10434–10438.

[45] Cho HJ, Jeong HG, Lee JS, Woo ER, Hyun JW, Chung MH, and You HJ (2002). Oncogenic H-Ras enhances DNA repair through the Ras/phosphatidylinositol 3-kinase/Rac1 pathway in NIH3T3 cells. Evidence for association with reactive oxygen species. *J Biol Chem* **277**, 19358–19366.

[46] Lee-Kwon W, Park D, and Bernier M (1998). Involvement of the Ras/extracellular signal-regulated kinase signalling pathway in the regulation of ERCC-1 mRNA levels by insulin. *Biochem J* **331**(pt 2), 591–597.

[47] Yacoub A, McKinstry R, Hinman D, Chung T, Dent P, and Hagan MP (2003). Epidermal growth factor and ionizing radiation up-regulate the DNA repair genes XRCC1 and ERCC1 in DU145 and LNCaP prostate carcinoma through MAPK signaling. *Radiat Res* **159**, 439–452.

[48] Shintani S, Li C, Mihara M, Terakado N, Yano J, Nakashiro K, and Hamakawa H (2003). Enhancement of tumor radioresponse by combined treatment with gefitinib (Iressa, ZD1839), an epidermal growth factor receptor tyrosine kinase inhibitor, is accompanied by inhibition of DNA damage repair and cell growth in oral cancer. *Int J Cancer* **107**, 1030–1037.

[49] McKenna WG, Weiss MC, Endlich B, Ling CC, Bakanauskas VJ, Kelsten ML, and Muschel RJ (1990). Synergistic effect of the v-myc oncogene with H-ras on radioresistance. *Cancer Res* **50**, 97–102.

[50] Sklar MD (1988). The ras oncogenes increase the intrinsic resistance of NIH 3T3 cells to ionizing radiation. *Science* **239**, 645–647.

[51] Saal LH, Gruvberger-Saal SK, Persson C, Lövgren K, Jumppanen M, Staaf J, Jönsson G, Pires MM, Maurer M, Holm K, et al. (2008). Recurrent gross mutations of the *PTEN* tumor suppressor gene in breast cancers with deficient DSB repair. *Nat Genet* **40**, 102–107.

[52] Shen WH, Balajee AS, Wang J, Wu H, Eng C, Pandolfi PP, and Yin Y (2007). Essential role for nuclear PTEN in maintaining chromosomal integrity. *Cell* **128**, 157–170.

[53] Baker SJ (2007). PTEN enters the nuclear age. *Cell* **128**, 25–28.

[54] Minami D, Takigawa N, Takeda H, Takata M, Ochi N, Ichihara E, Hisamoto A, Hotta K, Tanimoto M, and Kiura K (2013). Synergistic effect of olaparib with combination of cisplatin on PTEN-deficient lung cancer cells. *Mol Cancer Res* **11**, 140–148.

[55] Cancer Genome Atlas Network (2012). Comprehensive molecular portraits of human breast tumours. *Nature* **490**, 61–70.

[56] Natarajan S, Hombach-Klonisch S, Droge P, and Klonisch T (2013). HMGA2 inhibits apoptosis through interaction with ATR-CHK1 signaling complex in human cancer cells. *Neoplasia* **15**, 263–280.

[57] Wallin JJ, Edgar KA, Guan J, Berry M, Prior WW, Lee L, Lesnick JD, Lewis C, Nonomiya J, Pang J, et al. (2011). GDC-0980 is a novel class I PI3K/mTOR kinase inhibitor with robust activity in cancer models driven by the PI3K pathway. *Mol Cancer Ther* **10**, 2426–2436.

[58] Lee SJ, Lee SH, Yoon MH, and Park BJ (2013). A new p53 target gene, *RKIP*, is essential for DNA damage–induced cellular senescence and suppression of ERK activation. *Neoplasia* **15**, 727–737.

[59] Chakrabarty A, Sánchez V, Kuba MG, Rinehart C, and Arteaga CL (2012). Feedback upregulation of HER3 (ErbB3) expression and activity attenuates antitumor effect of PI3K inhibitors. *Proc Natl Acad Sci USA* **109**, 2718–2723.

[60] Yi YW, Hong W, Kang HJ, Kim HJ, Zhao W, Wang A, Seong YS, and Bae I (2013). Inhibition of the PI3K/AKT pathway potentiates cytotoxicity of EGFR kinase inhibitors in triple-negative breast cancer cells. *J Cell Mol Med* **17**, 648–656.

[61] Vijapurkar U, Robillard L, Zhou S, Degtyarev M, Lin K, Truong T, Tremayne J, Ross LB, Pei Z, Friedman LS, et al. (2012). mTOR kinase inhibitor potentiates apoptosis of PI3K and MEK inhibitors in diagnostically defined subpopulations. *Cancer Lett* **326**, 168–175.

EC50s of GDC-0980 in TNBC Cells

TNBT Cell lines	EC50s GDC-0980	*p53* Levels /Mutational status[2,] /*p53* (IS) [4] /TP53 Amino Acid Mutations[13]	PI3kinaseCA Mutation /PTEN Protein/*pten* Mutation[13]/ *Ras* (KRAS. HRAS) Mutation	*BRCA1* Mutation status	Epithelial / Mesemchymal Phenotype
HCC70*	0.46 μM	++M[2] /+++[4] / TP53 WT[13]	PI3KCA-WT[13]/ PTEN mutation[1] PTEN-Null [8,13] / PTEN WT[13] /RAS WT[13]		
HCC1143*	1.2 μM	++M[2] /+++[4] /TP53 WT[13]	PI3KCA-WT[13]/ PTEN-WT[8,13] / RAS WT[13]		
HCC1937*	3.75 μM	[-][2] / -[4] TP53 R306X[12]	PI3KCA-WT[13]/ PTEN-Null[8,10,13] /PTEN WT[13] / RAS WT[13]	Mutated[3] 5382insC[9]	Epithelial[5]
MDA-MB231*	5 μM	++M[2] / TP53 R280K[13]	PI3KCA-WT[13]/PTEN WT[8,10,13] /[KRas(G13D)][11,13]/BRAF(G464V)[13]	WT[9]	Mesenchymal[5]
MDA-MB468*	0.9 μM	[+] [2] /TP53 R273H[13]	PI3KCA-WT[13]/ PTEN mutation[1] PTEN-Null[8,10,13] /PTEN WT[13] /RAS WT[13]	WT[9]	Epithelial
BT20*	0.2 μM	++WT[2]	PIK3CA H1047R/ P539R[1] /PTEN-WT[8,10]	WT[9]	Epithelial[5]

*, From ATCC; ¶, Provided by Steve Ethier; Asterand
(http://www.cancer.med.umich.edu/breast_cell/Production/index.html
P53 protein levels and mutational status (M, mutant protein; WT, wild-type protein)
P53 Levels / Mutational status of the tumors used to derive the cell lines. Square brackets indicate mRNA levels (without any available protein data)[2] P53 (IS), P53 immuno-staining[4].
[1,] Gorden Mills 2006; [2,] Joe Gray 2006; [3,] C. Perou 2001; [4,] Adi Gazdar 1998; [5,] Lipkowitz 2008; [6,] Berkeley National lab; [7,] Steve Ethier, Asterand; [8,] Hoeflich et al. 2009; [9,] Elstrodt et al. 2006; [10,] Saal et al. 2006, 2008.[11,] Kozma SC, Bogaard ME, Buser K, et al The human c-Kirsten ras gene is activated by a novel mutation in codon 13 in the breast carcinoma cell line MDA-MB231. Nucleic Acids Res, 15: 5963-71, 1987.[Abstract/Free Full Text] [12,] Kraus MH, Yuasa Y, Aaronson SA. A position 12-activated H- ras oncogene in all HS578T mammary carcinosarcoma cells but not normal mammary cells of the same patient. Proc Natl Acad Sci USA, 81: 5384-8, 1984. [Abstract/Free Full Text] [13,] Hu et al Mol. Can. Res. 2009;7, 511-522 [14,] Lynn B. Eckert... Channing J. Der, Cancer Research 64, 4585-4592, July 1, 2004; [15] Chen et. al., 2009

Figure W1. EC_{50} of GDC-0980 in TNBC cell lines. Genetic backgrounds of the cells were tabulated.

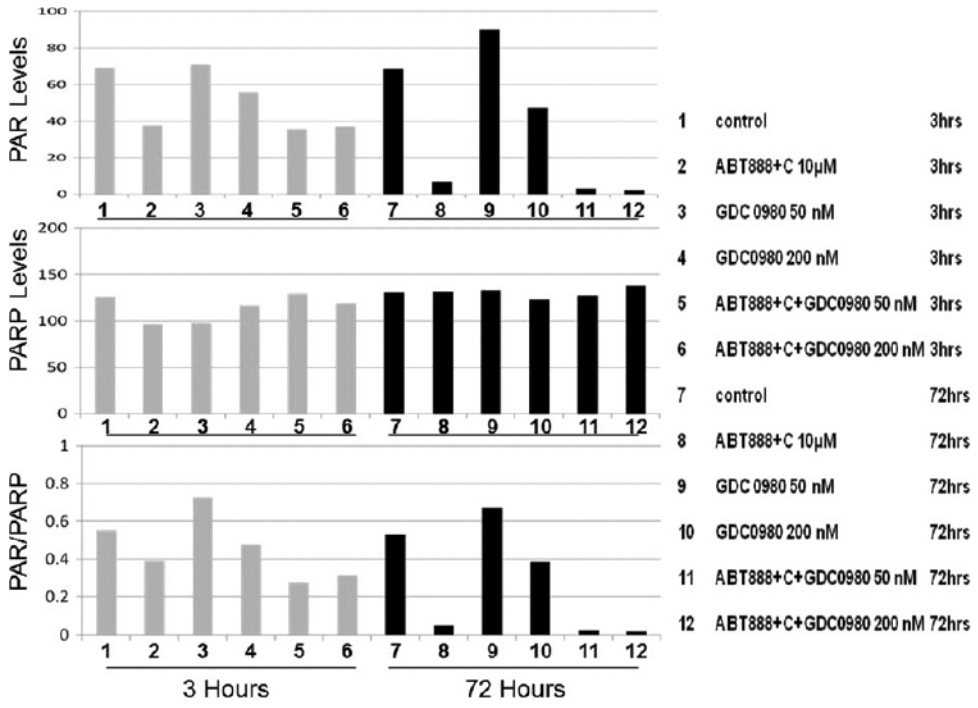

Figure W2. Effect of GDC-0980 alone and in combination with ABT888 plus carboplatin on ratios of PAR/PARP levels in MDA-MB231 at different time points. The semi-quantification of expression levels (of ImageJ intensities of the protein expression) of cellular PAR (upper panel), total PARP (middle panel), and ratio of PAR to total PARP (lower panel) in MDA-MB231 cells before and after treatments at different time points (3, 24, and 72 hours in successive darker shades) was shown as bar diagrams.

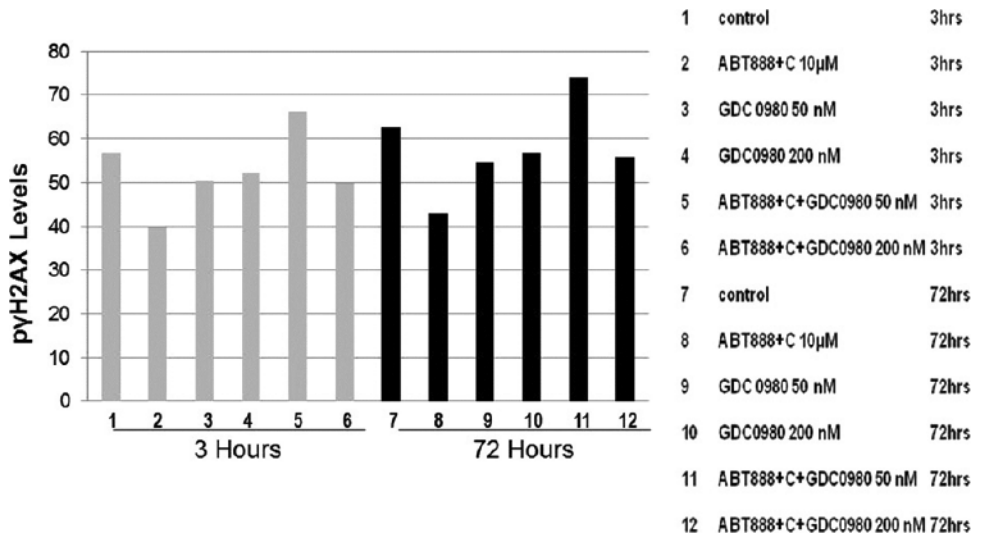

Figure W3. Effect of GDC-0980 alone and in combination with ABT888 plus carboplatin on pγH2AX^{S139} levels in MDA-MB231 at different time points. The semi-quantification of expression levels (of ImageJ intensities of the protein expression) of cellular pγH2AX^{S139} levels in MDA-MB231 cells before and after treatments at different time points (3 and 72 hours in successive darker shades) was shown as bar diagrams.

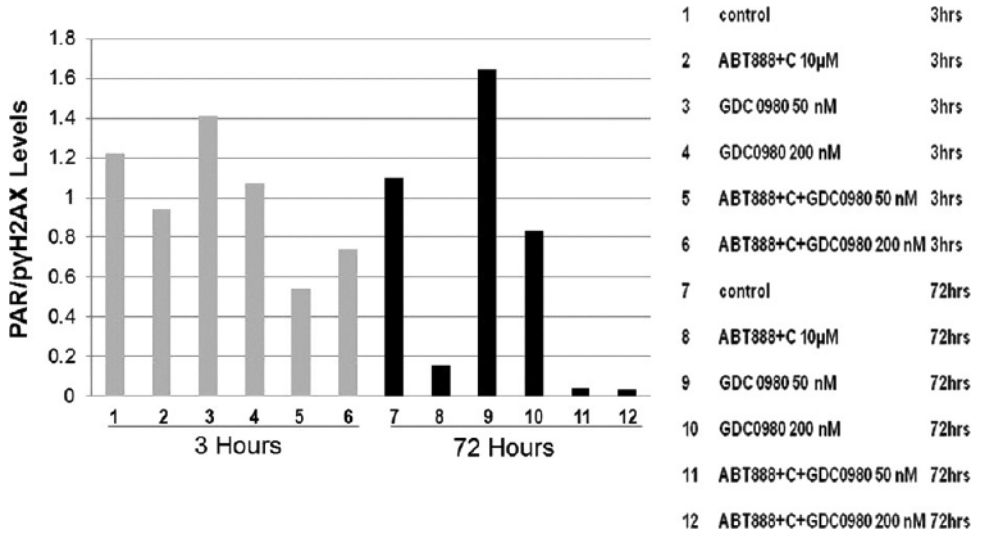

Figure W4. Effect of GDC-0980 alone and in combination with ABT888 plus carboplatin on ratios of PAR/pγH2AX^{S139} levels in MDA-MB231 at different time points. The semi-quantification of expression levels (of the ImageJ intensities of protein expression) of ratios of cellular PAR/pγH2AX^{S139} levels in MDA-MB231 cells before and after treatments at different time points (3 and 72 hours in successive darker shades) was shown as bar diagrams.

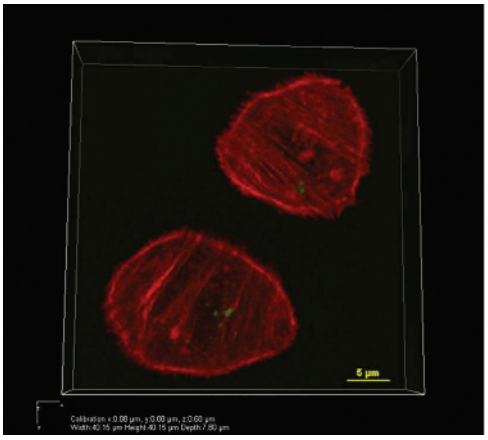

Movie W1. Three-dimensional projection movie showing nuclear pγH2AX^{S139} foci in vehicle-treated MDA-MB468 cells at 24 hours.

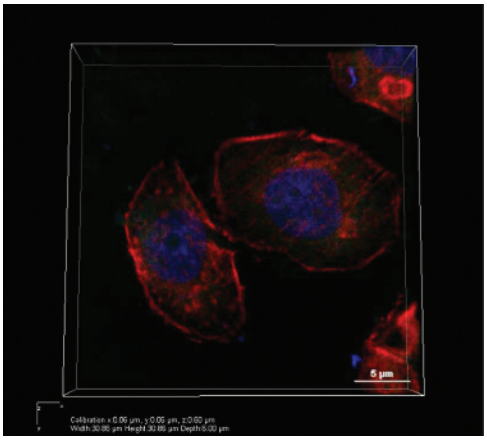

Movie W3. Three-dimensional projection movie showing the absence of cytoplasmic cleaved caspase 3 in vehicle-treated MDA-MB468 cells at 72 hours.

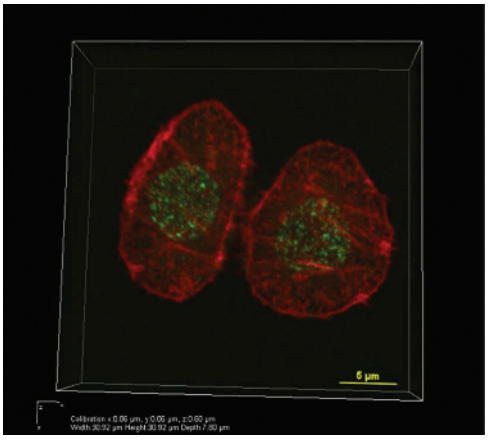

Movie W2. Three-dimensional projection movie showing the effect of GDC-0980 alone on nuclear pγH2AX^{S139} foci in MDA-MB468 cells at 24 hours.

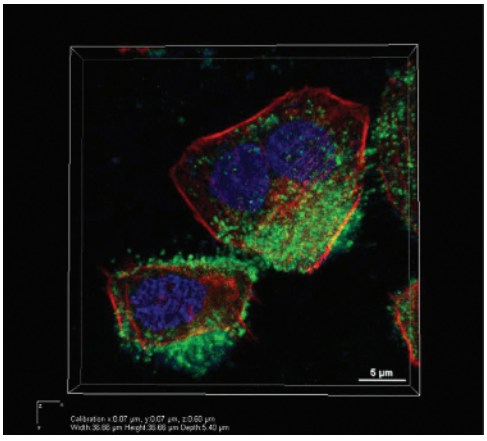

Movie W4. Three-dimensional projection movie showing abundance of cytoplasmic cleaved caspase 3 in GDC-0980 + ABT888 + carboplatin–treated MDA-MB468 cells at 72 hours.

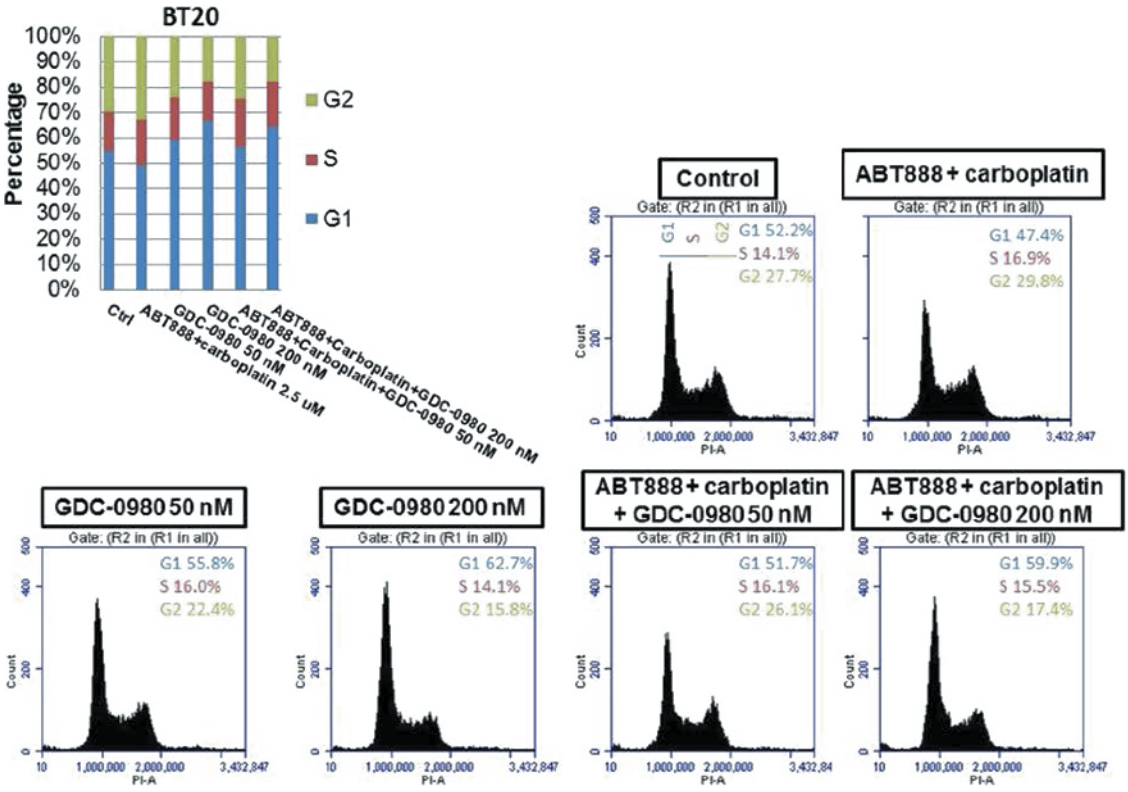

Figure W5. Effect of GDC-0980 alone and in combination with ABT888 plus carboplatin on cell cycle progression in BT20. Effect of two doses of GDC-0980 (50 and 200 nM) alone or in combination with ABT888 plus carboplatin (2.5 μM) on cell cycle progression after 24 hours in BT20 cells.